FINNISH METEOROLOGICAL INSTITUTE
CONTRIBUTIONS

No. 156

Application of remotely-sensed cloud properties for climate studies

Giulia Saponaro

Institute for Atmospheric and Earth System Research/Physics
Faculty of Science
University of Helsinki
Helsinki, Finland

ACADEMIC DISSERTATION in Physics
To be presented, with the permission of the Faculty of Science of the University of Helsinki, for public criticism in Brainstorm auditorium at Dynamicum, Erik Pálmenin Aukio 1, on January 8th, 2020, at 12 o'clock noon.

Finnish Meteorological Institute
Helsinki, 2020

Author's Address: Atmospheric Radiation
Finnish Meteorological Institute
P.O. Box 503
FI-00101 Helsinki, Finland
e-mail: giulia.saponaro@fmi.fi

Supervisors: Professor Gerrit de Leeuw, Ph.D.
Atmospheric Radiation
Finnish Meteorological Institute, Finland

Senior Scientist Pekka Kolmonen, Ph.D.
Atmospheric Radiation
Finnish Meteorological Institute, Finland

Reviewers Professor Kari Lehtinen, Ph.D.
University of Eastern Finland, Finland

Scientist Seiji Kato, Ph.D.
Climate Science Branch - Langley Research Center
National Aeronautics and Space Administration, USA

Custos Professor Veli-Matti Kerminen, Ph.D.
Institute for Atmospheric and Earth System Research
University of Helsinki, Finland

Opponent Doctor Nicolas Bellouin,
Meteorology Department
University of Reading, UK

ISBN 978-952-336-086-0 (paperback)
ISBN 978-952-336-087-7 (pdf)
ISSN 0782-6117

Printing House
Edita Prima Oy
Helsinki, 2020

Acknowledgments

The research presented in this work has been carried out at the Finnish Meteorological Institute. Ari Laaksonen, Sami Romakkaniemi and Hannele Korhonen are acknowledge for providing the work facilities.
I am deeply grateful to Prof. Gerrit de Leeuw, who originally hired me as an undergraduate student and introduced me to optical remote sensing. Thank you Gerrit for the trust you placed in me and in my work.
I ackowledge the pre-examiners Dr. Seiji Kato and Prof. Kari Lehtinen for their valuable comments on this thesis.

Thank you to all my colleagues (and friends). In particular from the Atmospheric Radiation group (former Aerosol and Cloud Remote Sensing group) I would like to mention Timo Virtanen, Larisa Sogacheva and Antti Arola for the good scientific collaboration, conversations and advices in a friendly environment. Additional and special thanks to Pekka Kolmonen, my supervisor, for his support during this PhD work.

I would like to thank my RI colleagues for cheering me trough this process to the finish line. In primis, the ACTRIS HO team: Sanna, Marjut, Eija, Anna, Niku, Silja, Edith, Päivi, Misha, Simo and Anniina.
Thank you Ulpu and Magdalena for the support, the great company during our trips and your friendship beyond work. Anca, every day I am grateful to share with you moment of joy, anger and muscles soreness.

I acknowledge the funding agencies and institutions that enabled me to attend international conferences and workshops during these years: the Maj and Tor Nessling foundation, the European Commission and, of course, the Finnish Meteorological Institute.

Finally, not by order of importance, I would like to thank my family for their support, encouragement and love. Thank you Antti for convincing me that anything is possible once you unlock what is between your ears. To my brother Andrea, thank you for the lunch-break phone calls. I owe my gratitude to my parents Enzo and Luigina: tutto ció che faccio é anche per voi.

ILMATIETEEN LAITOS
METEOROLOGISKA INSTITUTET
FINNISH METEOROLOGICAL INSTITUTE

Published by Finnish Meteorological Institute
(Erik Palménin aukio 1), P.O. Box 503
FIN-00101 Helsinki, Finland

Series title, number and report code of publication
Finnish Meteorological Institute
Contributions 156, FMI-CONT-156
Date
January 2020

Author
Giulia Saponaro

Title
Application of remotely-sensed cloud properties for climate studies

Abstract
Clouds play a vital role in Earth's energy balance by modulating atmospheric processes, thus it is crucial to have accurate information on their spatial and temporal variability. Furthermore, clouds are relevant in those processes involved in aerosol-cloud-radiation interactions. The work conducted and presented herein concentrates on the retrievals of cloud properties, as well as their application for climate studies. While remote sensing observation systems have been used to analyze the atmosphere and observe its changes for the last decades, climate models predict how climate will change in the future. Altogether, these sources of observations are needed to better understand cloud processes and their impact on climate. In this thesis aerosol and cloud properties from the three above mentioned sources are applied to evaluate their potential in representing cloud properties and applicability in climate studies on local, regional and global scales.

One aim of this thesis focuses on evaluating cloud parameters from ground-based remote-sensing sensors and from climate models using the MODerate Imaging Spectroradiometer (MODIS) data as a reference dataset. It is found that ground-based measurements of liquid clouds are in good agreement with MODIS cloud droplet size while poor correlation is found in the amount of cloud liquid water due to the management of drizzle. The comparison of the cloud diagnostic from three climate models with MODIS data, enabled through the application of a satellite simulator, helped to understand discrepancies among models, as well as discover deficiencies in their simulation processes. These findings are important to further improve the parametrization of atmospheric constituents in climate models, therefore enhancing the accuracy of climate projections.

In this thesis it is also assessed the impact of aerosol particles on clouds. Satellite data can be used to derive climatically crucial quantities that are otherwise not directly retrieved (such as aerosol index and cloud droplet number concentration) which can be used to infer the sensitivity of clouds to aerosols changes. Results on the local and regional scales show that contrasting aerosol backgrounds indicate a higher sensitivity of clouds to aerosol changes in cleaner ambient air and a lower sensitivity in polluted areas, further corroborating the notion that anthropogenic emission modify clouds. On the global scale, the estimates of the aerosol-cloud interaction present, overall, a good agreement between the satellite- and model-based values which are in line with the results from other models.

Publishing unit
Finnish Meteorological Institute

Classification (UDC)	Keywords	
591.543	Climate	
52-852	Atmosphere	
528.8	Remote sensing	
ISSN and series title		
0782-6117 Finnish Meteorological Institute Contributions		
ISBN	Language	Pages
978-952-336-086-0 (paperback), ISBN 978-952-336-087-7 (pdf)	English	62

Contents

List of publications

I G. Saponaro, P. Kolmonen, J. Karhunen, J. Tamminen, and G. de Leeuw, A neural network algorithm for cloud fraction estimation using NASA-Aura OMI VIS radiance measurements, *Atmospheric Measurement Techniques*, 6, 2301–2309, 2013.

II J. Preißler, G. Martucci, G. Saponaro, J. Ovadnevaite, A. Vaishya, P. Kolmonen, D. Cerburis, L. Sogacheva, G. de Leeuw, and C. O'Dowd, Six years of surface remote sensing of stratiform warm clouds in marine and continental air over Mace Head, Ireland, *Journal of Geophysical Research: Atmospheres*, 121, 14, 538–14, 557, 2016.

III G. Saponaro, P. Kolmonen, L. Sogacheva, E. Rodriguez, T. Virtanen and G. de Leeuw, Estimates of the aerosol indirect effect over the Baltic Sea region derived from 12 years of MODIS observations, *Atmospheric Chemistry and Physics*, 17, 4, 3133–3143, 2017.

IV G. Saponaro, M. K. Sporre, D. Neubauer, H. Kokkola, P. Kolmonen, L. Sogacheva, A. Arola, G. de Leeuw, I. H. H. Karset, A. Laaksonen, U. Lohmann, Evaluation of aerosol and cloud properties in three climate models using MODIS observations and its corresponding COSP simulator, and their application in aerosol-cloud interactions, *Atmospheric Chemistry and Physics Discussions.*

1. Introduction

Clouds play a key role in the climate system and are crucially important for climate change. As Earth's energy balance is determined by the amount of incoming shortwave solar radiation (sunlight) and the outgoing longwave radiation (mid- and thermal-infrared) emitted from the surface and the atmosphere, clouds can alter this balance and affect the Earth's climate system in a variety of ways (Stephens, 2005). Clouds can both absorb and reflect solar radiation, cooling the Earth's surface, and absorb and emit longwave radiation, warming the Earth's surface (Wallace and Hobbs, 2006; Seinfeld and Pandis, 2006; Lamb and Verlinde, 2011; Lohmann et al., 2016) as shown schematically in Fig.1.

The competition between these effects is regulated by the characteristics of clouds, such as cloud height, thickness, and radiative properties (Painemal, 2018; Goldblatt and J. Zahnle, 2011; Aebi et al., 2017). The complexity of clouds and their interactions with solar radiation represent the greatest difficulties in quantifying the effects of clouds on climate and in future projections of climate change (Flato et al., 2013). Clouds can rapidly transport air, energy, moisture, trace gases and aerosol particles from near the surface to the upper level of the atmosphere, hence quickly changing the composition and status of atmosphere. Moreover clouds are the source of precipitation and greatly regulate its distribution and amount (Lamb and Verlinde, 2011; Lohmann et al., 2016; Sun et al., 2018).

Thanks to the advances in remote sensing technologies, nowadays it is possible to accurately monitor clouds and other atmospheric constituents on local to global scales (Zhu et al., 2018). Remote sensing instruments do not directly measure the parameter of interest, for example cloud fraction, instead they detect the electromagnetic radiation transmitted, scattered, or emitted (radiance) in a given portion of the atmosphere. This electromagnetic radiation carries information about the atmosphere, and the role of a retrieval (or inversion) algorithm is to extract this information from the measurement and derive

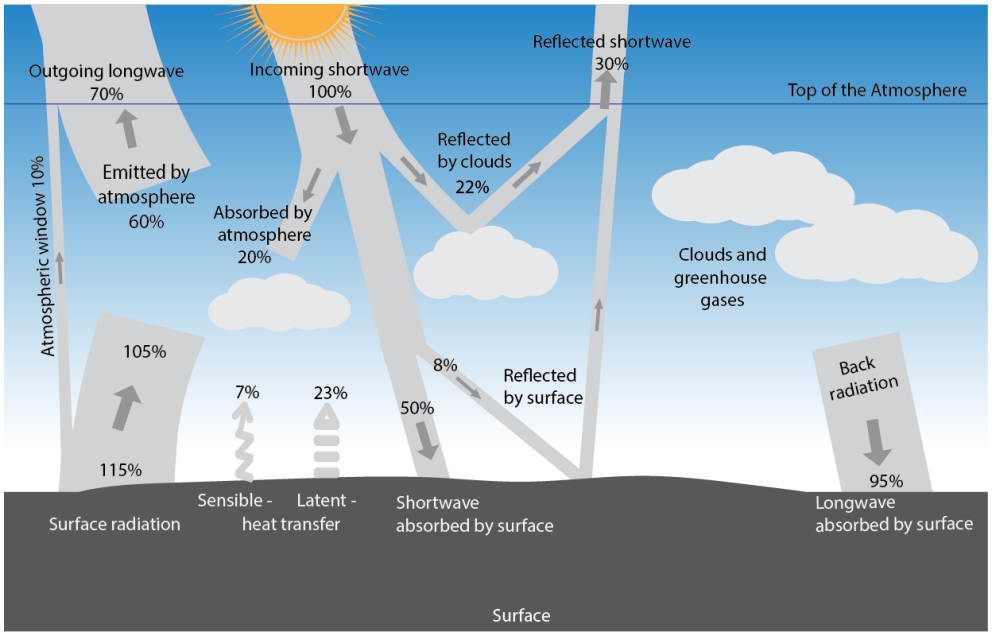

Figure 1: A schematic representation of Earth's radiation balance drawn after (Lamb and Verlinde, 2011).

the state and composition of the atmosphere. In other words, retrieval algorithms are developed to deduce properties of atmospheric constituents from the measured radiance and provide the relevant physical value (retrieval) through a suitable inversion method and an accurate forward model (inverse theory) (Huang et al., 2005).

Global data sets of cloud properties are routinely gathered using satellites, such as MODIS (Moderate Resolution Imaging Spectroradiometer), POLDER (Polarization and Anisotropy of Reflectances for Atmospheric science coupled with Observations from a Lidar), CALIPSO (Cloud-Aerosol Lidar and Infrared Pathfinder Satellite Observation), OMI (Ozone Monitoring Instrument) or AATSR (Advanced Along Track Scanning Radiometer). The traditional approaches to cloud detection (Rossow and Garder, 1993; Ackerman et al., 1998; Hulley and Hook, 2008; Hagolle et al., 2010; Heidinger et al., 2012; Zhu and Woodcock, 2014; Parmes et al., 2017) are based on the fact that the clouds tend to appear brighter and colder than the land surface. These methods imply difficulties in detecting clouds above bright (highly reflective) surfaces, such as snow, ice and deserts, because they mislead the retrieval algorithms to interpret the high measured reflectance as if it was reflected by clouds. The

detection of clouds is addressed in **Paper I** of this thesis. To this end the capability of artificial neural networks (ANN) for detecting clouds is tested using radiances measured at the top of the atmosphere with the NASA-Aura Ozone Monitoring Instrument (OMI). Besides providing cloud coverage, cloud detection is a necessary step in the retrieval of almost any atmospheric parameter from remote sensing data in the ultraviolet (UV), visible (VIS) or infrared (IR) parts of the electromagnetic spectrum (Eresmaa, 2014; Go et al., 2017; Nilo et al., 2018). Satellite observation of aerosols and clouds over the Baltic Sea countries are used in **Paper III** to study how contrasting atmospheric backgrounds (i.e. clean Fennoscandia and more polluted Central-Eastern Europe) impact upon clouds.

Satellite data are often complemented by ground-based observations which are also used as a reference in the validation for space-borne measurements (Marchand, 2016; Virtanen et al., 2018; Filonchyk et al., 2019). Unlike space-borne sensors, ground-based remote sensing provides continuous vertically resolved observations at one location. Although generally reliable, the accuracy of ground-based measurements is strictly dependent on the adopted inversion method. The retrieval algorithm SYRSOC (SYnergistic Remote Sensing Of Clouds) is applied in **Paper II** to derive microphysical and optical cloud properties of stratiform water clouds using the remote sensing suite at Mace Head, Ireland. The measurements are compared to MODIS and AATSR satellite retrievals.

Apart from the remotely-sensed observations, a branch of atmospheric science focuses on the development of representation of cloud processes in global climate models (Flato et al., 2013). Climate models represent a powerful tool for investigating the response of the climate system to various forcings as they enable climatic forecasts from seasonal to decadal timescales and for estimating projections of the future climate over the coming centuries (Collins et al., 2013; Christensen et al., 2013; Kirtman et al., 2013). Hence, the evaluation of modeling diagnostics is a crucial task that establishes the capabilities and reliability of models. **Paper IV** focused on this task and it presents the evaluation of three three climate models with MODIS cloud products.

By using remote sensing and models, the aims of this thesis are to:

- explore the capabilities and limitations of artificial neural networks for estimating cloud fraction (**Paper I**)
- compare cloud retrievals from ground-based algorithms and satellite data (**Paper II**)

- use satellite data to evaluate cloud diagnostics from climate models trough the application of satellite simulators (**Paper IV**)
- quantify the aerosol-cloud interactions and determine any contrasting results for heavily polluted areas against those for very clean areas (**Paper III** and **Paper IV**)

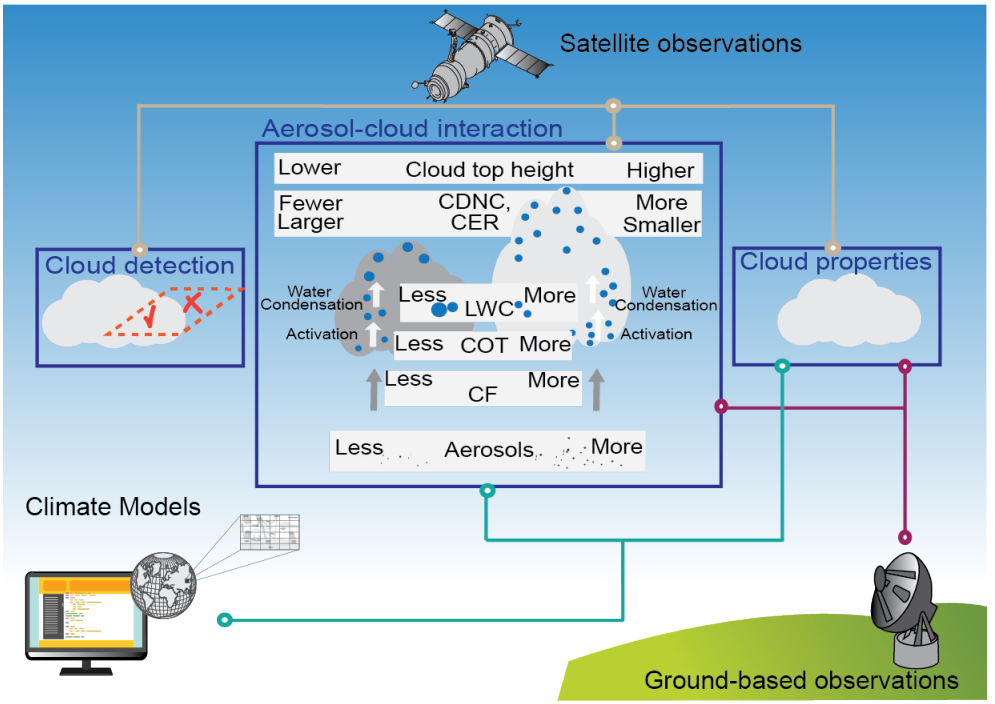

Figure 2: Schematic summary of the topics (cloud detection, cloud properties and aerosol-cloud interactions) and methods (satellite and ground-based observations, models) used in this thesis.

The introductory section of this thesis is structured as follows: Sect.2 briefly introduces the basics of clouds, aerosol and their interaction and Sect.3 presents the research methods, which are illustrated in Fig.2. Section 4 presents the main findings of this work and conclusion and future step are summarized in Sect.6.

2. Background

2.1. Light propagation through the atmosphere

Electromagnetic waves propagating through the atmosphere encounter gas molecules, aerosol particles, cloud droplets and ice crystals which modify the incident radiation by complex processes. The incoming radiation can be partly reflected or reradiated, changing the direction of propagation (scattering), and partly disappear by converting energy in heat or chemical energy (absorption). Overall, absorption and scattering processes define how solar and terrestrial radiation propagates through the atmosphere.

The nature of the interaction between electromagnetic waves and atmospheric constituents depends on the wavelength λ of the radiation and on the size distribution of the constituents (Bohren and Huffman, 2007). The absorption and scattering properties of homogeneous spherical particles with sizes comparable to λ can be derived using the Mie theory (Mie, 1908) which relates λ to the size and the chemical composition of the object.

After travelling a path of length z, the beam of light is attenuated following the Beer-Lambert law (Seinfeld and Pandis, 2006; Bohren and Huffman, 2007):

$$\frac{I(\lambda)}{I_0(\lambda)} = \exp(-\sigma_{\mathrm{e}}(\lambda)z) \tag{1}$$

where I_0 is the intensity of the incoming solar light at a wavelength λ, I is the intensity of the light at a wavelength λ at a location z along the path and σ_{e} is the extinction coefficient of the medium at a wavelength λ. The σ_{e} has three main components:

- Rayleigh scattering by air molecules, which occurs when the size of the air molecules is $< 1/10$ of the λ of I_0.
- Scattering and absorption by atmospheric aerosol particles, which is discussed in more details in Sect.2.2.
- Molecular absorption, whose main contributions are molecular oxygen and ozone, which strongly absorb radiation in the ultraviolet, and water, which strongly absorbs infrared radiation.

In the atmosphere solar radiation interacts with atmospheric constituents (aerosol, clouds and gases), all of which can absorb and/or scatter the radiation in certain spectral bands. The contributions from these various atmospheric

constituents interacting with the radiation are additive (Wallace and Hobbs, 2006). Therefore, the total $\sigma_{\mathrm{E}}(\lambda)$ accounts for aerosol, clouds and gases:

$$\begin{aligned}\sigma_{\mathrm{e}}(\lambda) &= \Sigma_i \sigma_{\mathrm{e_i}} \\ &= \Sigma_i \sigma_{\mathrm{a_i}} + \Sigma_i \sigma_{\mathrm{s_i}} \\ &= \Sigma_i \sigma_{\mathrm{ag_i}}(\lambda) + \sigma_{\mathrm{sg_i}}(\lambda) + \sigma_{\mathrm{ap_i}}(\lambda) + \sigma_{\mathrm{sp_i}}(\lambda) + \Sigma_i \sigma_{\mathrm{ac_i}}(\lambda) + \sigma_{\mathrm{sc_i}}(\lambda)\end{aligned} \tag{2}$$

where the first letter of each subscript represents either absorption (a) or scattering (s) and the second the contribution of gas (g), aerosol (p) and clouds (c). Furthermore, we can define $\Sigma_{\mathrm{i}}\sigma_{\mathrm{e_i}}$, $\Sigma_{\mathrm{i}}\sigma_{\mathrm{a_i}}$ and $\Sigma_{\mathrm{i}}\sigma_{\mathrm{s_i}}$ as (Wallace and Hobbs, 2006):

$$\sigma_{\mathrm{e}}(\lambda) = \Sigma_{\mathrm{i}}\sigma_{\mathrm{e_i}} = \Sigma_{\mathrm{i}}\rho_{\mathrm{i}}\mathrm{K}_{\mathrm{e_i}} = \Sigma_{\mathrm{i}}\mathrm{N}_{\mathrm{i}}\mathrm{K}_{\mathrm{e_i}} \tag{3}$$

$$\sigma_{\mathrm{a}}(\lambda) = \Sigma_{\mathrm{i}}\sigma_{\mathrm{a_i}} = \Sigma_{\mathrm{i}}\rho_{\mathrm{i}}\mathrm{K}_{\mathrm{a_i}} = \Sigma_{\mathrm{i}}\mathrm{N}_{\mathrm{i}}\mathrm{K}_{\mathrm{a_i}} \tag{4}$$

$$\sigma_{\mathrm{s}}(\lambda) = \Sigma_{\mathrm{i}}\sigma_{\mathrm{s_i}} = \Sigma_{\mathrm{i}}\rho_{\mathrm{i}}\mathrm{K}_{\mathrm{s_i}} = \Sigma_{\mathrm{i}}\mathrm{N}_{\mathrm{i}}\mathrm{K}_{\mathrm{s_i}} \tag{5}$$

where ρ_{i} and N_{i} are the density and particle (for example aerosol) number concentration, respectively, of the ith constituent and K is the (dimensionless) extinction efficiency.

The total amount of radiation scattered by particles for a given medium in any direction is a function of particle composition and size. The composition determines the particle absorption properties. Particles that are very small compared to λ are scattering radiation in the Rayleigh regime, in which scattering efficiency is $\mathrm{K} \propto \lambda^{-4}$, therefore very effective at short wavelengths (e.g. at UV and the blue end of the visible spectrum), the scattering is divided evenly between the forward and backward direction of the radiation propagation. When particle size is comparable to λ, the Mie regime, radiation propagates preferentially along the forward-scattering direction while geometric optics apply when particles are much larger than λ (Lamb and Verlinde, 2011).

2.2. Aerosol

Minuscule liquid and solid particles suspended in the atmosphere, known as aerosol particles, can be found mainly in the closest three kilometers to Earth's surface (Tian et al., 2017; Koffi et al., 2016). Aerosol particles can enter the atmosphere directly in a particle form (i.e. dust, sea salt, pollen, organic compounds) or they can form in the atmosphere as a result of reactions between gaseous compounds in a process known as nucleation (Kazil et al., 2010; Kulmala et al., 2012). The diameter of aerosol particles ranges from 1-2 nm for freshly formed molecular clusters (Kulmala et al., 2013) to 100 μm for dust or pollen, for example. Fine aerosol, with radius between 0.1 μm and 1 μm,

can grow by condensation, where gaseous molecules condense on the particle surface, or coagulation, where smaller fine aerosols collide and stick together.

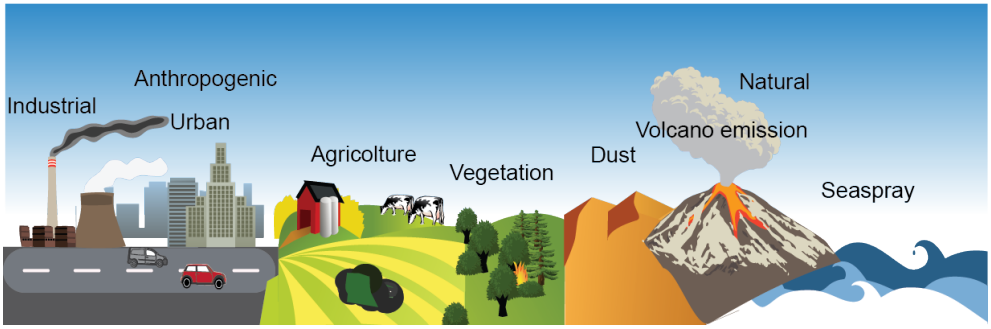

Figure 3: Examples of anthropogenic and natural sources of aerosol particles.

The Earth's atmosphere contains various types of aerosol particles (Fig.3) with different concentrations and chemical compositions originating from biological sources (i.e. spores, seeds, pollen, sea salt, smoke from wild fires), solid Earth (i.e. volcano emissions, dust), anthropogenic processes (dust from roads, biomass burning, fuel combustion, industrial activities) and in-situ formation due to condensation of gases (i.e. gas to particle conversion from precursor gases such as sulfuric acid bases and volatile organic compounds) (Wallace and Hobbs, 2006; Kalberer, 2015; Tegen and Schepanski, 2018; Hoesly et al., 2018).

Once emitted, aerosol particles are transported by the wind over long distances. Their residence time in the atmosphere varies from few days to weeks (Fig.4), depending on the particle size, until they are removed from the atmosphere by precipitation, gravitation, cloud processing, collision with larger particles or by sticking onto existing surfaces (i.e vegetation) (Kristiansen et al., 2012; Bellouin and Haywood, 2015).

Aerosol particles can be described by their physical properties, such as size, size distribution and shape, their chemical composition and optical properties, such as extinction, scattering and absorption coefficients (Hansen and Travis, 1974).

The single scattering albedo w_0 defines the scattering and absorption fractions of $\sigma_e(\lambda)$:

$$w_0 = \frac{\sigma_s}{\sigma_s + \sigma_a} \tag{6}$$

The aerosol optical depth (AOD) is one of the most common aerosol optical parameters is retrieved from aerosol remote sensing instruments, for example MODIS (Fig. 4 and 5) and AERONET sunphotometers, and it is related to

Figure 4: A true-color image from the Moderate Resolution Imaging Spectroradiometer (MODIS) over Northern Italy, on March 17, 2005. Northern Italy is a highly populated and industrialized area. The the Alps block the transport of the air between northern Italy and the rest of Europe and large amount of air pollution can accumulate in the air even for days. Therefore, it often happens that the sky in the Po valley area appears hazy: this phenomena is captured in the satellite snapshot and it can be clearly observed by human eye. From the image hazy skies extend over the Po Valley and reach the Adriatic sea. Credit: Jeff Schmaltz, MODIS Land Rapid Response Team. Reprinted with permission from NASA Goddard Space Flight Center.

the amount of aerosol in the vertical column of the atmosphere in the observed direction. It is defined as:

$$\mathrm{AOD}(\lambda) = \int_0^{\mathrm{TOA}} \sigma_{\mathrm{e_p}}(\lambda, z)\mathrm{d}z \tag{7}$$

where the extinction coefficient $\sigma_{\mathrm{e_p}}$ accounts for aerosol absorption and aerosol scattering $\sigma_{\mathrm{e_p}} = \sigma_{\mathrm{a_p}} + \sigma_{\mathrm{s_p}}$ and AOD is the integrated $\sigma_{\mathrm{e_p}}$ over the total atmospheric column, i.e. from the surface $z = 0$ to the top of the atmosphere $z =$ TOA.

The Ångström exponent (AE) describes the wavelength dependency of the AOD (Ångström, 1929):

$$\mathrm{AE} = -\frac{\log\frac{\mathrm{AOD}\lambda_1}{\mathrm{AOD}_{\lambda_2}}}{\log\frac{\lambda_1}{\lambda_2}} \tag{8}$$

and qualitatively indicates the aerosol particle size (Ångström, 1929; Moosmüller et al., 2009; Dhar et al., 2018; Lack and Langridge, 2013). Values of AE ≤ 1 are indicative of coarse particles, i.e. dust and sea salt, whereas values of AE≥ 2 indicate the presence of fine particles, typically associated with urban pollution or biomass burning (Shin et al., 2019; Zotter et al., 2017; Lack and Langridge, 2013).

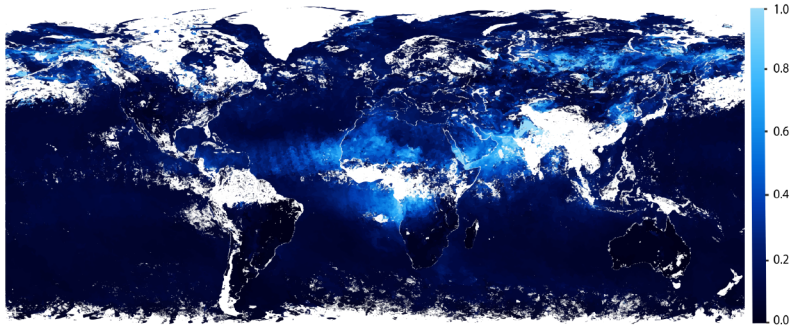

Figure 5: Monthly averaged (July 2019) AOD from MODIS/Aqua. Light blue pixels show high aerosol concentrations, while dark blue pixels show lower concentrations, and black areas show little or no aerosols. white shows where aerosol properties could not be retrieved. The image is produced using the science data set Level 2 AOD 550 Dark Target Deep Blue Combined regridded at a 0.1 degrees spatial resolution. Credit: original imagery by Reto Stockli, NASA's Earth Observatory, using data provided by the MODIS Atmosphere Science Team, NASA Goddard Space Flight Center. Modified and reprinted with permission from NASA Goddard Space Flight Center.

Depending on the the aerosol optical (determined by chemical composition) properties, aerosols can scatter or absorb the shortwave and thermal radiation. Scattering aerosols exert a cooling effect of the atmosphere, whilst absorbing aerosol particles cause a local warming of the atmosphere at the level at which they are located (Bellouin, 2015). In the recent Intergovernmental Panel on Climate Change's (IPCC) Fifth Assessment Report (AR5) (Boucher et al., 2013) these processes are called Radiative Forcing from Aerosol-Radiation Interaction (RFari). Additionally, aerosols indirectly affect climate by altering cloud properties, such as albedo, droplet size, cloud radiation properties, and precipitation (Lohmann, 2006; Rosenfeld, 2006). For example, absorbing aerosol can modify the evaporation rate of cloud droplets and warm the atmosphere, hence hindering or enhancing cloud production, and consequently affecting precipitation (Lee, 2012; Rosenfeld and Givati, 2006; Zhou et al., 2017; Stjern et al., 2017).

Aerosols may also act as cloud condensation nuclei CCN (Aitken, 1881) or ice nuclei IN (DeMott et al., 1997), which are an indispensable element in cloud formation and a relevant factor affecting cloud properties. Not all aerosols are activated into CCN or IN and their activation strongly depends on their size, chemical composition and mixing state.

2.3. Clouds

Clouds are the place in the atmosphere where water passes from its gaseous phase (water vapour) to its liquid and/or solid phase. Clouds consist of microscopic droplets of liquid water (warm clouds), ice crystals (cold clouds), or both (mixed-phase clouds). Their mean droplet radius is typically in the range 10-20 μm for liquid clouds and 25-35 μm for ice clouds, a remarkable size difference in comparison to raindrops and snowflakes which we all can see without any equipment (Fig.6).

Clouds forms as a result of saturation of the air. The air is saturated when the liquid and vapour phases are in equilibrium, the temperature is equal to the dew point and the relative humidity is 100%. Saturation is reached either by mechanisms cooling the air to its dew point or by adding moisture to the air (Lamb and Verlinde, 2011).

When saturated air cools, for example via adiabatic cooling of an air parcel by updrafts, the water vapour concentration exceeds the equilibrium value below the dew point and the air becomes supersaturated. In this condition, the supersaturated air can no longer contain the same amount of water vapor and condensation may occur. Aerosol particles are a indispensable element in cloud formation because they facilitate the conversion of water vapour into its

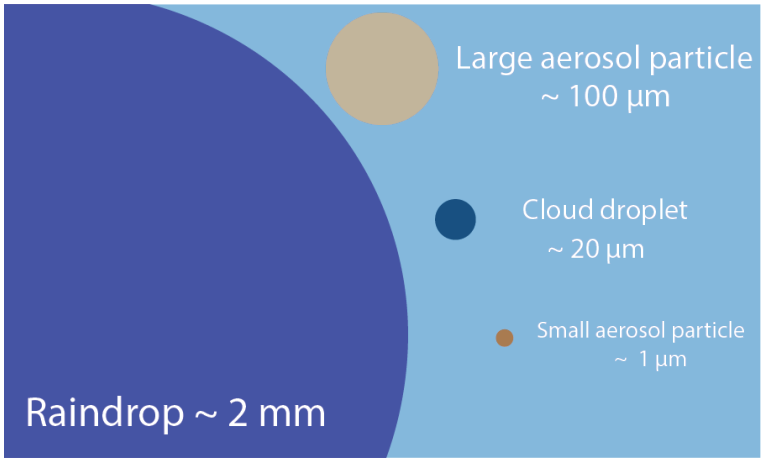

Figure 6: Comparison of typical sizes of aerosols, cloud droplet and raindrop.

liquid (rain) and/or solid phase (ice crystals) by acting as a preferred surface on which water vapour condense. For this reason, aerosol particles acting as condensation surfaces are referred to as cloud condensation nuclei (CCN). The ability of aerosol particles to activate as cloud droplets depends on aerosol properties (i.e. size and hygroscopicity) and on the meteorological conditions (i.e. water vapour, temperature and velocity updraft).

When enough vapour condenses onto the CCN and the supersaturation of the air exceed a critical value according to Kölher theory, a cloud droplet is formed (Köhler, 1936). The Kölher theory describes how the supersaturation and the critical diameter for the cloud drop activation depend upon the size and chemical composition of CCN. It indicates that as the supersaturation increases, the size at which particles can be activated decreases. In other words, the higher is the hygroscopicity and size of the particle, the lower is the required supersaturation level for cloud droplet formation (Köhler, 1936; Kulmala et al., 1996; Reutter et al., 2009; Mochida et al., 2011; Väisänen et al., 2016).

However, condensational growth alone is not enough to form rain droplets and ice-crystals. Other processes, such as collision-coalescence, riming and aggregation, are responsible for precipitation events: if droplets collide with a sufficient number of other droplets, they grow by collection into precipitation-sized droplets and reach the surface in form of rain droplets or ice-crystals.

Clouds cover roughly two thirds of the globe (Mace et al., 2009), as shown in Fig.7). The mid-latitude oceanic storm tracks and tropical precipitation belts are particularly cloudy, while continental desert regions and the central

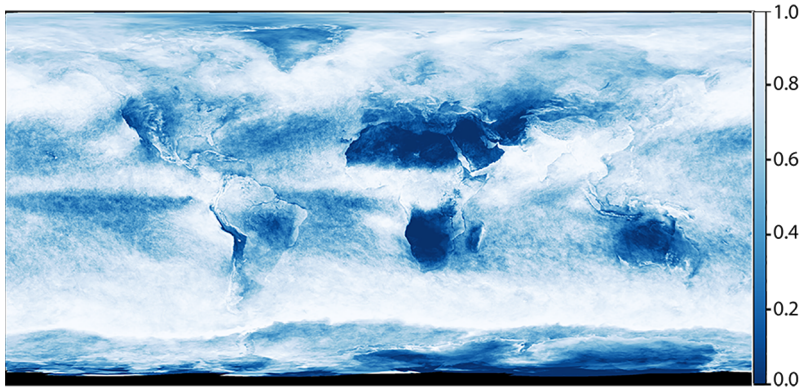

Figure 7: Monthly averaged (July 2019) cloud fraction from MODIS/Aqua. Cloud fraction is the portion of each pixel that is covered by clouds. Colors range from blue (no clouds) to white (totally cloudy). The image is produced using the scientific data set CloudFraction derived from the 1-km-pixel resolution Cloud Mask product. Credit: original imagery by Reto Stockli, NASA's Earth Observatory, using data provided by the MODIS Atmosphere Science Team. Modified and reprinted with permission from NASA Goddard Space Flight Center.

subtropical oceans are relatively cloud-free. At any given time, most clouds are not precipitating (Sun et al., 2018).

In this thesis I adopt from Boucher et al. (2013) the commonly used vertical classification of clouds that considers 'high' cloud above the 440 hPa pressure level, 'low' below the 680 hPa and in between 'mid-level'. High clouds (i.e. cirrus and deep cumulus) are mainly distributed near the equator and over tropical continents, but they also occur in the mid-latitude storm track regions and over mid-latitude continents in summer. Mid-level clouds occur prominently in the storm tracks and, less frequently, in the Intertropical Convergence Zone (ITCZ). Low-level clouds are seen over mainly over oceans (Boucher et al., 2013; Mace et al., 2009; Chepfer et al., 2010).

Clouds directly condition the transmission of sunlight and infrared radiation in the atmosphere, consequently the temperature of Earth, and ultimately climate, by scattering and absorbing incoming solar radiation and outgoing longwave radiation (see Figure 1).

In general, the role of clouds on climate depends on their altitude and thickness (Yan et al., 2016; Hang et al., 2019; L'Ecuyer et al., 2019). High-level clouds, such as cirrus clouds, consists of ice and reflect little sunlight but efficiently trap infrared light emitted from Earth's surface. Low-level clouds, and to some extent mid-level clouds, such as stratus clouds strongly reflect

incoming solar radiation and weakly impact on the outgoing infrared radiation, while cumulus clouds can block sunlight but also trap the Earth's heat depending on their heights and thicknesses. The overall effect of clouds on climate is a cooling effect because the amount of solar radiation reflected back to space by clouds is higher than the amount of infrared radiation emitted by clouds towards the surface (Hartmann, 1993; Boucher and Quaas, 2007; Lamb and Verlinde, 2011).
The cloud properties used in this thesis are introduced in Sect.3.

2.4. Aerosol-cloud interactions

As mentioned in the previous sections, aerosol particles and clouds play a key role in the processes regulating Earth's radiative budget. The recent Intergovernmental Panel on Climate Change (IPCC)'s Fifth Assessment Report (5AR) (Boucher et al., 2013) indicates the interactions between aerosols, clouds and radiation as the largest key climate uncertainty. Therefore, it is crucial to improve the level of understanding of the effects of aerosol, clouds and their interactions on atmospheric processes.

The nomenclature describing the aerosol-cloud-radiation interactions has been changing throughout the years and the IPCC 5AR (Boucher et al., 2013) introduced a new terminology, shown in Fig.8, to describe the two main mechanism perturbing Earth's radiation balance:

- the radiative forcing due to aerosol-radiation interactions (RFari) encompasses what was previously referred to as the aerosol direct effects and characterize the effect of aerosol particles interacting directly with incoming sunlight or emitted thermal radiation through scattering and absorption processes;

- the radiative forcing due to aerosol-cloud interactions (RFaci) comprises what was previously known as the aerosol first indirect effect and describes any change to the Earth's radiative budget due to the modification of cloud microphysical properties by aerosols.

The term aerosol-cloud interactions may be used in its most broad meaning to refer to any interaction between aerosol and clouds (Bellouin et al., 2019). However, in this thesis it is quantified by the metric ACI which defines the change in an observable cloud property (e.g., cloud optical depth, cloud effective radius, cloud droplet number concentration) to a change in a cloud condensation nuclei proxy (e.g. aerosol optical depth, aerosol index, or aerosol particle number concentration). If LWP is assumed to be constant

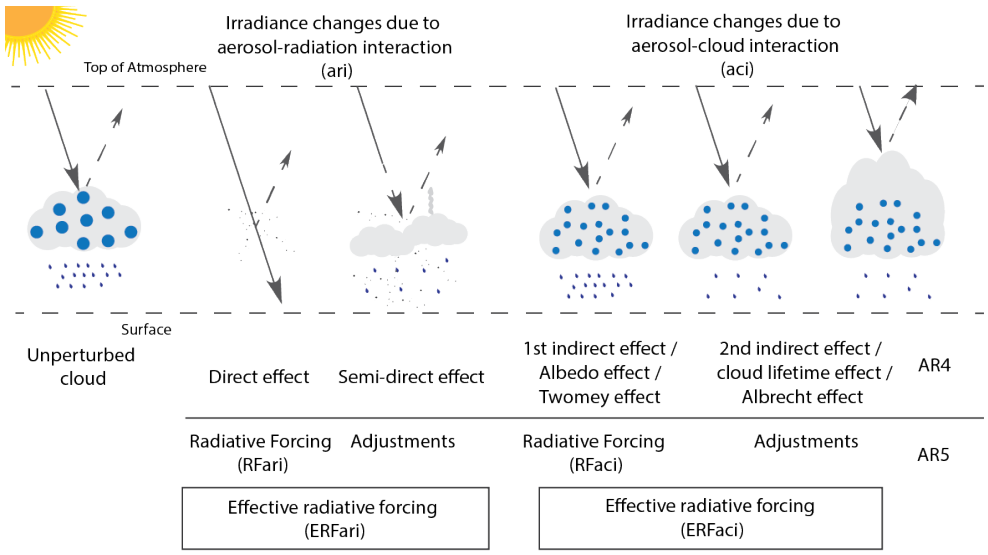

Figure 8: Schematic summary of the interactions between radiation, aerosol and clouds. The nomenclature adopted in the IPCC AR4 (Forster et al., 2007) is now being replaced by the new terminology presented in the recent IPCC AR5 (Boucher et al., 2013)

and additional CCN are inserted in a shallow warm cloud, a higher number of CCN compete for the same amount of liquid water amount, leading to a larger number cloud droplets of smaller size than the same cloud in unperturbed conditions. Consequently, the total surface area of the cloud droplets is larger, more solar radiation is reflected back to space, making the cloud brighter, and less radiation reaches the surface as the optical thickness of the cloud increases. This effect is also known as the Twomey effect or cloud albedo effect or first indirect effect (Twomey, 1977).

Furthermore, smaller droplets may also decrease the frequency of precipitation, consequently increasing the cloud lifetime (Albrecht, 1989) and cloud coverage (Kaufman and Koren, 2006). The term adjustments is used nowadays to indicate these processes (Boucher et al., 2013).

A widely-used approach to the assessment of ACI parameter is to follow the methodology introduced by Feingold et al. (2003) and attribute perturbations in a selected cloud property to changes in the chosen cloud condensation nuclei proxy:

$$\mathrm{ACI} = \frac{\mathrm{d}\ln(\delta)}{\mathrm{d}\ln(\sigma)} \tag{9}$$

where δ is the observed cloud property (COT, CER, LWP or CDNC) and σ the CCN proxy, as CCN are not a measurable quantity for most instrument techniques (i.e. for satellite instrumentation). Aerosol loading is often used as a proxy (Andreae, 2009) which is usually expressed by the aerosol optical depth (AOD) or the aerosol index (AI), derived as the product of AOD × ÅE, or the Fine Mode AOD (AODf), the part of the total AOD which is contributed by fine mode aerosol particles.

It is important to highlight that using AOD as a surrogate of CCN implies the following shortcomings:

- AOD from satellite observations are limited for aerosol particles with diameter larger then 0.1 μm (Seinfeld et al., 2016);
- high relative humidity causes aerosols to swell and create difficulties in deriving size distributions (Neubauer et al., 2017; Liu and Li, 2018);
- AOD measurements may be biased due to cloud contamination or cloud obstruction (Koren et al., 2008; Yang et al., 2014; Zhu et al., 2015);
- AOD is a total column measurement which does not provide any information regarding the proximity to clouds nor about the aerosol size distinction nor the aerosol type (Stier, 2016);

Next, some of the challenges and limitations in assessing ACI are highlighted. AOD retrievals are limited to cloud-free conditions, which creates challenges to studying the ACI where the intention is to study collocated aerosol and cloud observations. Unless height-resolving instruments (i.e. lidars) are considered, the vertical location of the AOD level is unknown. Aerosol and cloud measurements may contain retrieval errors, which are further propagated to ACI estimates, as well as they reciprocally may bias the respective retrievals (Jia et al., 2019). The interpretation of the observed aerosol-cloud relationships is complicated by the effect of meteorology (Quaas et al., 2010; Gryspeerdt et al., 2014, 2016; Brenguier et al., 2003). As cloud formation happens in high humidity conditions, aerosol humidification can severely affect the assessment of ACI by causing positive correlation between AOD and cloud properties (Myhre et al., 2007; Quaas et al., 2010; Grandey et al., 2013; Gryspeerdt et al., 2014). Additionally to aerosol particles, water vapour also affects precipitation (Boucher et al., 2013), obviously linked to the presence of clouds, and consequently causes spurious correlations between aerosols and clouds (Koren et al., 2012).

This thesis tackles the assessment of the ACI by using remote sensing observations and global modeling of warm liquid stratiform clouds deriving estimates

of ACI from local to global scales. Many studies derived ACI estimates from local to global scales using in-situ (Werner et al., 2014) and ground-based (Qiu et al., 2017) measurements, satellite observations (Ma et al., 2018) or modeling approaches (Gryspeerdt et al., 2017), or a combination of modeling diagnostics and observations (Ban-Weiss et al., 2014). The advances in the level of understanding are, however, limited by the intrinsic limitations of each approach (Seinfeld et al., 2016; Lohmann et al., 2016; Bellouin et al., 2019).

3. Data & methods

The goal of studying Earth's atmospheric constituents is to improve the understanding of atmospheric processes. A deeper knowledge on atmospheric composition enables advances in monitoring and improving air quality as well as in predicting future climate responses to changes in natural and anthropogenic emissions. Observations from satellite instruments, ground-based measurements and model diagnostics are fundamental tools for monitoring the atmosphere.

3.1. Space-borne remote sensing

3.1.1. MODIS retrievals

The Moderate Resolution Imaging Spectrometer (MODIS) is a 36-channel radiometer flying aboard the Terra and Aqua satellites since 2000 and 2002, respectively. MODIS views the entire Earth's surface every 1 to 2 days, thus providing an extensive data set of global Earth observations. MODIS delivers a wide range of atmospheric products including aerosol and cloud properties, water vapour and atmospheric stability variables.

MODIS Level-1 (L1) products are geo-located brightness temperature values, which are converted to geophysical data products at Level-2 (L2) using retrieval algorithms, which can be aggregated into a uniform space-time grid at Level-3 (L3).

The 1-km (at nadir) spatial resolution MODIS cloud mask is the basis of MODIS aerosol and cloud retrievals. The cloud mask provides the probability for a given pixel to be influenced by the occurrence of clouds, classifying the pixels as confident clear, probably clear, uncertain–probably cloudy or cloudy. Pixels falling in the former two groups are used for retrieving aerosol properties. The latter two classes are labeled as cloudy when calculating cloud fractions (Platnick et al., 2015).

The L2 aerosol products are provided over land (except over ice and snow) and ocean surfaces for cloud-free conditions during daytime at a nominal spatial resolution of 10 x 10 km^2 (Levy et al., 2015). The primary aerosol product is AOD retrieved globally at the wavelength of 550 nm, while the other parameters accounting for the aerosol size distribution, such as AE, defined in Eq.8, or fine-mode AOD, are only derived over ocean (Levy et al., 2013).

The L2 cloud parameters include cloud top properties (e.g. cloud amount, top temperature, pressure, emissivity, and height) and physical and optical properties (e.g. particle phase, effective particle size, optical thickness, water

path, fraction) under both daytime and nighttime conditions with a 1 x 1 km^2 resolution (for Collection 6 onwards) (Hubanks et al., 2018). Cloud fractions are derived at 5-km resolution by calculating the proportion of cloudy pixels from 25-pixel cloud mask groupings.

The cloud droplet effective radius (CER or r_e) is a measure of the cloud droplet size and it is defined as (Hansen and Travis, 1974):

$$\mathrm{CER} = r_e = \frac{\int_0^\infty r_e^3 n(r) \mathrm{d}r}{\int_0^\infty r_e^2 n(r) \mathrm{d}r} \tag{10}$$

where $n(r)$ is the cloud droplet size distribution.

Simultaneously to CER, the cloud optical thickness (COT) is derived. CER and COT are retrieved coupling the MODIS-measured reflectances in one of the visible (non-absorbing) channels and one near-infrared or infrared band (water-absorbing channels) by using look-up tables, which are created by a radiative transfer model calculating the amount of reflection produced by clouds characterized by a range of COT and CER as a function of the wavelength (Platnick et al., 2018). The look-up table approach has the following limitations:

- the determination of CER becomes uncertain at low COT (Cho et al., 2015; Zhang et al., 2012);
- the algorithm assumes single-layered liquid water clouds with plane-parallel geometry, which do not realistically represent all clouds, especially convective clouds. Furthermore, the plane-parallel assumption becomes weaker for low solar zenith angles (Grosvenor and Wood, 2014).
- Cloudy pixels are either defined as liquid or ice clouds, whereas most of the clouds in the atmosphere with temperature between -6 °C and -38 °C are mixed-phase clouds.

The liquid water path (LWP), the amount of liquid water per unit volume of air, is derived from the CER and COT as (Han et al., 1998)

$$\mathrm{LWP} = \frac{4\rho_\mathrm{w}}{3K_e} \mathrm{COT} \cdot \mathrm{CER} \tag{11}$$

where $\rho_\mathrm{w} = 1$ g cm-3 is the water density and $\mathrm{K_e} \approx 2$ is the extinction efficiency in the visible band used for the retrieval of COT and CER (King et al., 1997). Equation (8) presumes vertically homogeneous clouds in combination with cloud top effective radius retrievals (Borg and Bennartz, 2007).

Furthermore, three different products of the cloud properties introduced above are produced using three different water absorbing channels (1.6 μm, 2.1 μm and 3.6 μm). Zhang et al. (2012) showed that CER retrieved at 3.6 μm is less sensitive to the plane-parallel cloud assumption.

The geolocated L2 MODIS atmospheric products are aggregated in L3 onto a regular $1^\circ \times 1^\circ$ grid and averaged over a day, 8-days and a month span (Hubanks et al., 2018). In addition to the nominal atmospheric variables, L3 MODIS products come along with a suite of statistical quantities derived from the corresponding L2 data product.

The cloud droplet number concentration (CDNC), the number of water droplets in a volume of cloud, can be derived from CER and COT by combining Eqs. (6) and (9) from Bennartz (2007), resulting in the following equation:

$$\mathrm{CDNC} = \gamma \cdot \mathrm{COT}^{0.5} \cdot \mathrm{CER}^{-2.5} \tag{12}$$

where $\gamma = 1.37 \cdot 10^{-5}$ m$^{0.5}$ (Quaas et al., 2006). The assumption of not accounting for temperature effect and setting γ as a bulk costant applies rather well to the warm stratiform clouds in the marine boundary layer but less for convective clouds (Bennartz, 2007; Rausch et al., 2010; Grosvenor et al., 2018). The equation represents the "Idealized Stratiform Boundary Layer Cloud" (ISBLC) model (Bennartz and Rausch, 2017) which is based on the following assumptions:

- the cloud is horizontally homogeneous
- the LWC increases linearly from the cloud base to the cloud top
- the CDNC is constant throughout the vertical extent of the cloud

While the ISBLC model describes important aspects of stratiform boundary layer clouds, its assumption will never be fully valid for any real cloud. Issues related to the ISBLC model assumptions are extensively elaborated in Bennartz (2007); Bennartz and Rausch (2017) and references therein. However, compared to the methodology of Bennartz (2007), we use the revised and improved cloud retrievals from MODIS Collection 6 (Platnick et al., 2015, 2017).

MODIS cloud properties retrieved at 3.6 μm are used in **Paper II** and **Paper III**, while the standard 2.1 μm was used in **Paper IV** to match the wavelength used in the COSP-MODIS simulation. MODIS L2 cloud properties are used in **Paper I** and **Paper II** and MODIS L3 data are applied in **Paper III** and **Paper IV**. In **Paper II** and **Paper III**, transparent-cloudy pixels (COT < 5) were discarded to limit uncertainties (Zhang et al., 2012). MODIS L2 aerosol data are used in **Paper III** and L3 in **Paper IV**.

3.1.2. OMI retrievals

The Ozone Monitoring Instrument (OMI) is a near-UV-visible spectrometer flying on NASA's Aura satellite since 2004. OMI measures radiance at 751 wavelengths in the UV/VIS domain and it has a nominal spatial resolution of 13 $\times$ 24 km^2 at nadir, in the normal global operation mode. Complete global coverage is achieved daily (Levelt et al., 2006) between 2002 and 2008, while after 2008 the global coverage is achieved in two days due to the row anomaly (Yan et al., 2012), which affects the quality of OMI radiance data. By monitoring the global total column ozone, absorbing and non-absorbing aerosol loading, trace gases and clouds, OMI's measurements contribute to studying the recovery of the ozone layer, the sources of aerosols and trace gases affecting air quality, UV surface fluxes and climate change. OMI's radiances (Level-1b) are used in **Paper I**.

3.2. Ground-based remote sensing

Ground-based remote sensing enables continuous atmospheric observations at one location with high temporal and spatial resolution. These characteristics represent an advantageous asset for obtaining detailed insight in atmospheric processes. Ground-based techniques can be classified into active or passive ones, depending on their operational principles.

Active sensors emit electromagnetic radiation at a certain wavelength and measure the backscattered signal to study the properties of the observed target. A radar (RAdio Detection And Ranging) is a system that uses an electromagnetic wave in the radio or microwave domain. Radars operating with frequencies of 35 GHz (8 mm) or 94 GHz (3 mm) are known as cloud radars. Cloud radars are nowadays applied for determining cloud properties up to 10-15 km in altitude and high temporal resolution (1-10 s). As longer wavelengths are less sensitive to drizzle and rain while shorter wavelengths may be attenuated by smaller particles, cloud radars' application extends from the detection of hydrometeors to fog, giant aerosols and insects. A radar sample may contain several targets with different vertical velocities and shapes. Individual targets can be distinguished with the application of Doppler spectra and linear depolarization ratio techniques which enable the detection of the signatures of different targets.

Ceilometers are a sub-category of the LiDAR (LIght Detection And Ranging) system which are configured to optimize cloud observations. They are smaller and less expensive than more powerful atmospheric Lidar systems (e.g. Doppler Lidars, Rayleigh Doppler radar), but follow the same work-

ing principle: a laser beam is sent vertically into the atmosphere where part of the signal is backscattered by atmospheric constituents (e.g. aerosol, clouds, gases) and the intensity of he backscattered radiation is collected by the lidar instrument. Depending on the working combination of wavelengths, the remote mapping of different atmospheric components is enabled by identifying wavelength-dependent changes in the intensity of the returned signal. Ceilometers can be used to determine cloud types, boundaries (e.g. cloud base, top height) and precipitation.

Complimentary to cloud radars and lidars, radiometers are passive sensors measuring the energy emitted at millimetre-to-centimetre wavelengths (frequencies of 1–1000 GHz), known as microwaves, which make the sensor very sensitive to the thermal electromagnetic radiation emitted by atmospheric gases.

In **Paper II** we use 6 years of data collected in Mace Head, at the west coast of Ireland, www.macehead.org./) from a CloudNet station consisting of two active sensors, a ceilometer and a cloud radar, and a passive sensor, a microwave radiometer. The radar reflectivity and microwave radiometer profiles of temperature and humidity as well as liquid water path measurements are input to the SYROC (SYnergistic Remote Sensing Of Clouds) algorithm, a software package developed at the National University of Ireland in Galway (NUIG), that calculates the profiles of CDNC, CER and LWC from the collocated cloud radar, ceilometer or lidar, and microwave radiometer data (Martucci and O'Dowd, 2011). The ground-based measurements processed by SYRSOC are evaluated with MODIS and AATSR in **Paper II**. While SYRSOC produces profiles of the microphysical cloud properties, MODIS has a limited penetration depth into clouds and mainly retrieves microphysical cloud properties near cloud top. SYRSOC CER, COT and integrated LWC were averaged about 10 min before and 10 min after the overpass. MODIS values with COT < 5 were discarded. Additionally, measurements of aerosol composition from the ground-based in situ aerosol mass spectrometer (AMS) (Ovadnevaite et al., 2014) were also used in **Paper II**.

3.3. Climate models

Climate models represent a sophisticated tool for studying Earth's atmosphere and predicting climate change. A global atmospheric model schematically simulates Earth's atmosphere in a 3-dimensional grid. By solving the mathematical equations that describe the physical atmospheric processes, given initial conditions and parameters, models compute winds, heat transfer, radiation, relative humidity, and surface hydrology within each grid point.

One key limiting factor in the quality of climate predictions by current global atmospheric models is the realistic representation of the simulated properties (e.g. cloud cover, amount of cloud water, and number and size of droplets or ice crystals) that describe the atmospheric constituents (e.g. clouds).

The evaluation of modeling diagnostics is an important task that establishes the capabilities and reliability of models, hence it helps to improve the parametrization of modelled atmospheric variables. A robust evaluation of model diagnostics is not a straight-forward task: model-to-model and model-to-satellite intercomparison are affected by a number of limitations and incongruities intrinsic in the data. For example, the compensation of modeling errors, the uncertainties of observational data, and the possible discrepant definitions of variables between models and observational data are some of the major issues.

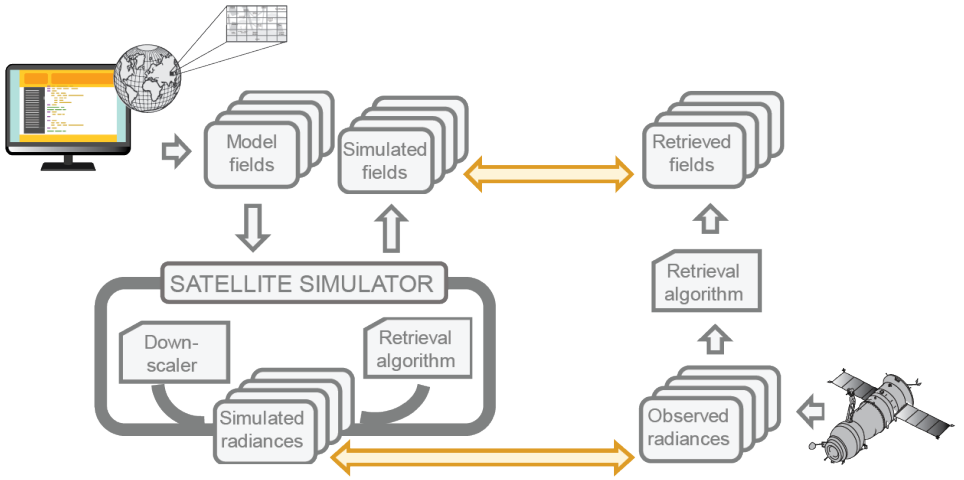

Figure 9: Schematic representation of the basic principle of COSP satellite simulator. COSP is a diagnostic tool that maps the model representation of clouds to synthetic satellite observations.

The application of a a satellite simulator, which mimics the retrieval of observational data, remedies these inconsistencies. In other words, simulators recreate what a satellite would retrieve when observing the modeled atmosphere, thus generating physical quantities fully consistent with satellite retrievals and preventing inconsistencies in the modelled outputs. Consequently, simulators represent a valuable approach not only for the application of satellite data to robustly evaluate models, but also for consistent model-to-model comparisons.

In **Paper IV** three climate models were considered, ECHAM-HAM, ECHAM-HAM-SALSA and NorESM, and in each of them the Cloud Feedback Model Intercomparison Project (CFMIP) Observation Simulator Package, COSP (Bodas-Salcedo et al., 2011) version 1.4 was implemented. COSP is a software tool developed within the CFMIP (Webb et al., 2017) which models parameters for several spaceborne active (CALIOP, CPR) and passive (MISR, MODIS) sensors (Fig.9). In our case we considered the COSP-MODIS simulator. One year of data (2008) of COSP-simulated liquid and ice cloud (CF, CER, COT, LWP) and aerosol (AOD and AI) properties was compared to MODIS L3 data. The COSP grid-averaged values were divided by the corresponding cloud fractions to match the MODIS in-cloud grid values. The model three-hour outputs were aggregated to daily averages and successively re-gridded and co-located by linear interpolation onto the finer satellite regular grid of 1°×1°. Furthermore, MODIS observations and MODIS-COSP diagnostics were screened using a minimum threshold of 30% of cloud fraction to minimize the source of errors introduced by the retrieval algorithm and to ensure the existence of large-scale clouds. Additionally to the MODIS-COSP diagnostics, I also considered the model direct outputs for CDNC which is representative of the entire vertical structure of a simulated atmospheric column. Top-column values were considered to maintain consistency with MODIS and MODIS-COSP values, which observe the top of the clouds, and they were screened for values with temperature T > 273°K to discard mixed-phase and ice clouds.

4. Overview of key results

4.1. Determination of cloud fraction

Cloud detection is a fundamental step for atmospheric observation, whether we aim to observe clouds themselves or other atmospheric constituents (Eresmaa, 2014; Go et al., 2017; Nilo et al., 2018). A faulty classification of clouds can cause an incorrect analysis of the observations.

The process of cloud detection relies upon the contrast between clouds and background (either atmosphere or surface) in the observed field (Ackerman et al., 2010). Different automated cloud detection techniques have been developed depending on the requirements of the application, for example the tolerance of the application to uncertainty in the cloud amount estimate. Cloud quantification can be deterministic providing binary products such as cloudy/cloud-free pixels (Rossow and Garder, 1993), multi-class categorical, for example cloudy, partial-cloud, cloud-free and unknown in Ackerman et al. (2010), or representative of a continuous measurement, i.e. the probability of cloud coverage or the probability of cloud-free as introduced in Aleksandrova et al. (2018).

Clouds are easily distinguishable from surface types other than snow and ice, due their high reflectivity of solar radiation at visible wavelengths. However, this distinction is limited to daytime when solar zenith angles are sufficiently large and the reflected sunlight provides enough contrast in the imagery. Many automated cloud detection approaches rely on tests using a combination of visible and infrared channels to determine the presence of clouds (Ackerman et al., 2010; Sun et al., 2017; Zhu et al., 2015). The success of these cloud test techniques depends on the determination of the thresholds used in each cloud test. The techniques which perform the best are usually the most complex and computationally heavy as they have several spectral tests and thresholds that vary with the geographic region, time of year, time of day and solar angle, for example.

In **Paper I**, a fast and automated neural networks-based solution was explored for determining cloud fraction. The method was designed specifically for the NASA Aura's satellite Ozone Monitoring Instrument (OMI) which observes back scattered solar radiation in the visible (VIS) and ultraviolet (UV), thus lacking the thermal channels. Two neural network (NN) algorithms, namely extreme learning machine (ELM) and back propagation (BP) algorithms, were developed and used to estimate cloud fractions using OMI radiance measurements from the visible channels. OMI data were divided into independent datasets for training, testing and validating the results from the neural net-

works. The results were evaluated by comparison with cloud fractions available from the MODerate Resolution Imaging Spectrometer (MODIS). OMI and MODIS both fly in the A-train constellation but on different platforms, respectively Aura and Aqua with a time difference of 15 minutes between the observations.

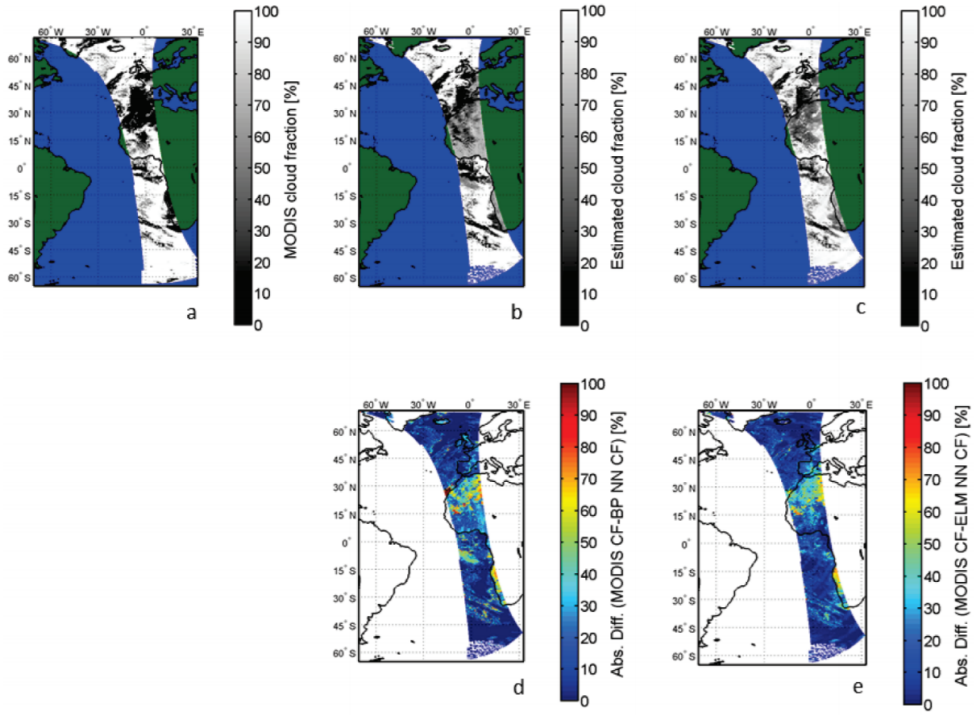

Figure 10: Cloud fractions estimated by the BP and ELM-trained NN and comparison with MODIS CF data for validation over a selected orbit. (a) Computed MODIS geometrical cloud fraction. (b) BP predicted cloud fraction. (c) ELM predicted cloud fraction. The grey-code in top-row figures (a-c) ranges from 0 (cloud free) to 100 (totally cloud covered). The bottom-row figures show the absolute difference between MODIS geometrical cloud fraction and BP-predicted cloud fraction (d) and ELM-predicted cloud fraction (e). The color-code ranges from 0 (perfect match) to 100 (complete mismatch).

Both neural networks were successfully implemented and delivered estimates of cloud fraction in a fast and automated way. However, the NNs showed limitation when estimating small cloud fractions, where the BP algorithm showed the worst results. The neural networks performed rather well in the evaluation with MODIS cloud fraction data. As the ocean provides a

homogeneous dark surface in the UV/VIS, hence providing a good contrast between cloudy and clear pixels, good correlations with R values of 0.85 and 0.88 are achieved over ocean, for ELM and BP, respectively. Over land, highly reflective surfaces, such as desert (Fig.10), or the presence of dust layers in the atmosphere, represented a challenge for the neural network and the cloud fractions were not well predicted. The ELM outperformed the BP algorithm with R values of 0.83 and 0.56, respectively, for ELM and BP.

4.2. Evaluation of cloud properties

4.2.1. Ground-based measurements and MODIS observations

Non precipitating single-layer homogenous water clouds data collected by the ground-based remote sensing instruments at the Mace Head Atmospheric Research Station from 2009 to 2015 were input into the SYRSOC algorithm to derive profiles of CER, LWC, and COT. A total of 118 stratiform clouds were identified and successively they were classified as marine or continental, based on three-day back-trajectories from the National Oceanic and Atmospheric Administration (NOAA) HYSPLIT model (HYbrid Single-Particle Lagrangian Integrated Trajectory) (Draxler and Rolph, 2014) and the synoptic conditions. 40 cases coincident with overpasses of the MODIS Aqua or Terra satellites over Mace Head were used for a comparison of the SYRSOC results with the corresponding MODIS products at 3.7 μm (Platnick et al., 2015).

MODIS data were selected and averaged over an area from 53.27 to 53.37 °N and from −9.91 to 9.89 °E, with Mace Head located at its center. MODIS pixels with COT < 5 were removed before averaging. SYRSOC produces profiles of the microphysical cloud properties. However, MODIS has a limited penetration depth into clouds and therefore only retrieves microphysical cloud properties near cloud top. Therefore, SYRSOC CER averaged from 75 m to 45 m below the radar detected cloud top, while LWP was integrated over the full cloud depth. SYRSOC CER, COT and integrated LWC were averaged over time from about 10 min before to 10 min after the MODIS overpass.

Comparison of SYRSOC results with MODIS observations shows a moderate correlation of CER (R=0.43), shown in Fig.11 a, and a rather poor agreement of COT (R=0.19). No correlation was found between the integrated SYRSOC LWC and MODIS LWP, shown in Fig.11 b. The SYRSOC algorithm discards measurements if drizzle is detected and this screening process discards cloud areas with high LWP, resulting in integrated values considerably lower than the MODIS LWP. LWP was also measured directly by the MWR and used as input for SYRSOC. Better agreement was found between the di-

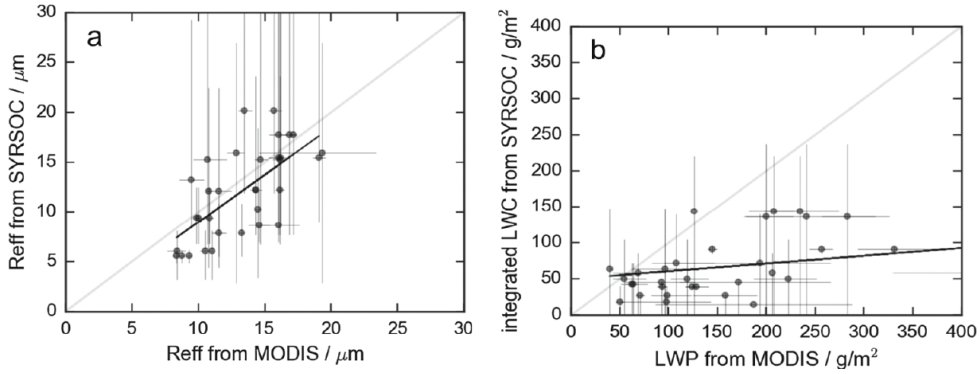

Figure 11: Comparison of (a) reff and (b) integrated LWC/LWP from MODIS and SYRSOC, including downdrafts and drizzle. Dots mark mean values, and error bars span minima to maxima. The 1:1 line and linear fit are shown in gray and black, respectively

rectly measured LWP and MODIS LWP than between SYRSOC results and MODIS products, with the exception of high-mean LWP, where the variability of both instruments was larger.

Integrated SYRSOC LWC was in many cases lower than MWR LWP. In order to investigate whether the LWP differences were caused by the drizzle screening, the SYRSOC run was repeated without drizzle screening. Agreement was improved by running SYRSOC without drizzle screening, which resulted in an increase of R2 for LWC from 0.04 to 0.14. Comparison of CER with drizzle resulted in a slope near 1 and a small offset of -1 μm. The correlation of COT was greater when drizzle was included. However, apart from CER with a slope near 1 and small offset, overall the comparison with MODIS data shows a poor agreement. Comparison with MODIS products at 1.6 μm and 2.1 μm showed similar results.

4.2.2. Model diagnostics and MODIS observations

The evaluation of modeling diagnostics with appropriate observations is an important task that establishes the capabilities and reliability of models. In this perspective, aerosol and cloud properties obtained from three different climate models, namely ECHAM-HAM, ECHAM-HAM-SALSA and NorESM, are considered.

Results for global means and geographical distributions of aerosol and cloud properties were assembled over a one-year period (2008) and compared with MODIS observations in **Paper IV** providing a quantitative evaluation of cloud

and aerosol diagnostics. Different results were obtained when considering liquid or ice clouds.

Significant biases are observed globally in NorESM ice clouds because NorESM includes radiatively active snow (Kay et al., 2012). The droplet size and water content of ice clouds are underestimated in ECHAM-HAM and ECHAM-HAM-SALSA possibly owing to the cirrus scheme which does not account for heterogenous nucleation or pre-existing ice crystals during formation of cirrus clouds (Lohmann and Neubauer, 2018; Neubauer et al., 2019).

Global differences can be also observed in liquid clouds (Figure 12). The droplet size (Figure 12 e-h) simulated by ECHAM-HAM around the mid-latitude belt are on average 5 μm smaller than in ECHAM-HAM-SALSA and NorESM, and ECHAM-HAM-SALSA simulates larger cloud droplets around the polar areas and shows a large positive bias for LWP over ocean in comparison to ECHAM-HAM. The liquid water path simulated by NorESM is larger over land areas while ECHAM-HAM shows a good agreement with MODIS (Fig.12 j-k).

Despite having identical cloud modules, the discrepancies between ECHAM-HAM and ECHAM-HAM-SALSA may originate from different amounts of activated droplets and different ice nucleation rates. The COSP diagnostics of liquid clouds CER and COT were successively used to derive the CDNC, following the approach presented in Quaas et al. (2006), and compared to the corresponding MODIS-derived values. Overall the MODIS derived CDNC is lower than that derived from COSP simulated values, but higher than the direct output values. Consequently, the CDNC from direct model output is lower than MODIS-COSP diagnostics, as also found by Ban-Weiss et al. (2014). Possible explanations could be either related to the COSP computation of cloud diagnostics or the approach itself used for deriving CDNC.

Considering the vertical distribution of the COSP-simulated clouds, both ECHAM-HAM and ECHAM-HAM-SALSA fail in simulating high level clouds while the vertical distribution of clouds simulated by NorESM is similar to MODIS.

The evaluation led to the identification of the following deficiencies in the models:

- the clouds simulated by NorESM are too thick over land and this issue is present in COSP-variables as well as in the direct model output due to a very low autoconversion parameter causing the suppression of precipitation over land, thus thicker clouds;
- ECHAM-HAM-SALSA systematically simulates lower IWC than ECHAM-HAM due to a higher cloud droplet freezing rate which con-

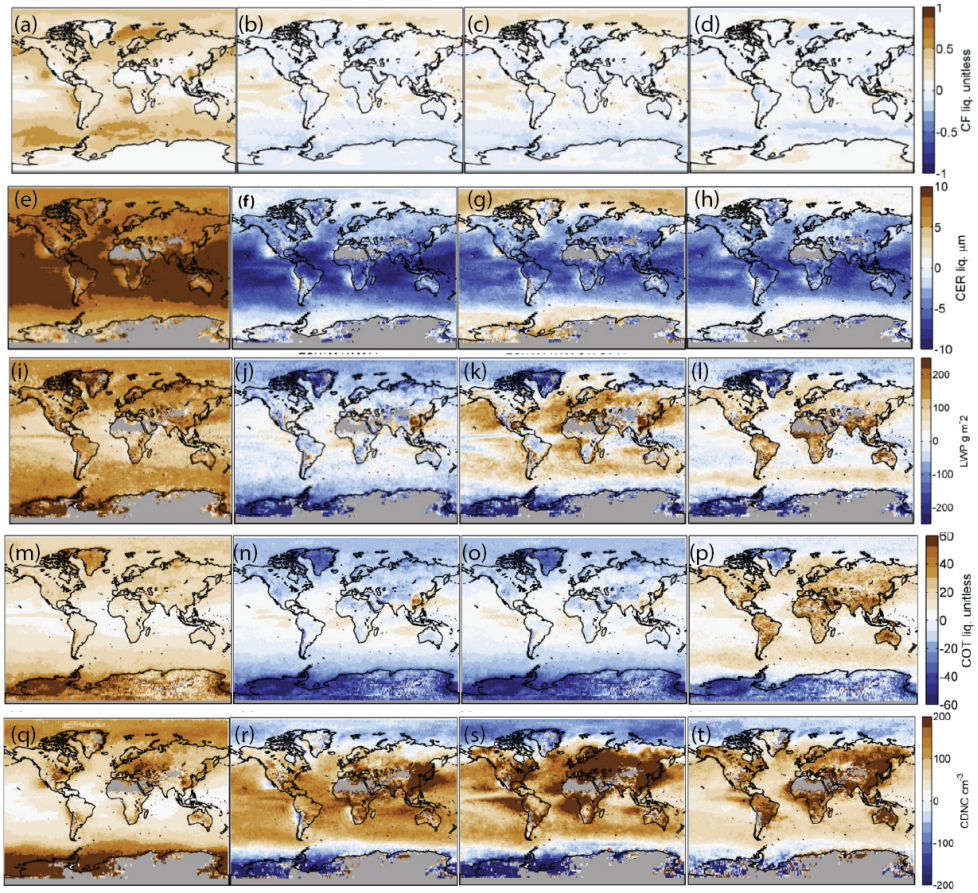

Figure 12: Annual global mean bias in the properties characterizing liquid warm clouds. The bias represents the difference calculated subtracting MODIS observation to MODIS-COSP diagnostics simulated by ECHAM-HAM, ECHAM-HAM-SALSA, and NorESM. The first image in each row presents MODIS spatial distributions as reference.

secutively triggers a reduced sedimentation of ice clouds. This outcome explains the contradictory result in ECHAM-HAM-SALSA that showed the largest global average among the models for CER despite having the highest numberof CDNC;

- the direct model output for CDNC is systematically larger than both the values derived from COSP-diagnostics and MODIS observations, supporting the results found Ban-Weiss et al. (2014).

4.3. Analysis of aerosol-cloud interactions

In this work the topic of aerosol-cloud interactions introduced in Sect.2.4 was studied using different measurement techniques (satellite observations, ground based measurements, modelling diagnostics) and approaches (spatial distribution, linear regression analysis, vertical profiling, air mass analysis) for different scales (local, regional and global).

Long-term analysis of ACI was conducted in **Paper II** and **Paper III**.
Six year measurements of remote sensing aerosol and cloud properties from Mace Head were studied in **Paper II**. The findings showed higher CDNC and lower CER during greater pollution events, confirming the Twomey effect. In marine air masses the median CDNC was 60 cm^{-3} and the median CER 10 μm. In continental air the median CDNC was 160 cm^{-3} and the median CER was 8 μm. Droplet size distributions were broader in marine cases and narrower in continental cases. Generally, clean air masses showed also lower COT and cloud albedo and higher values were found in more polluted conditions.
In **Paper III**, 12 years of aerosol and low-level liquid cloud properties were used to statistically quantify the ACI over the Baltic Sea region, including the relatively clean Fennoscandia and the more polluted central–eastern Europe. Changes in cloud structures were shown by the increase of CF, COT, LWP and CTH, and a decrease of CER as function of aerosol loading, especially at relatively low cloud-top levels, between 900 hPa and 700 hPa. Most of the studied cloud variables were unaffected by the lower-tropospheric stability (LTS), except for cloud fraction.
The ACI was studied as the change in CER as a function of aerosol concentration for fixed LWP bin values (Fig.13). Positive and statistically significant ACI values were found over the Baltic Sea and Fennoscandia, with the former having the largest values. Small negative ACI values were observed over central–eastern Europe, suggesting that large aerosol concentrations saturate the ACI and that a given change in aerosol number exerts a stronger effect in pristine regions than in polluted regions.

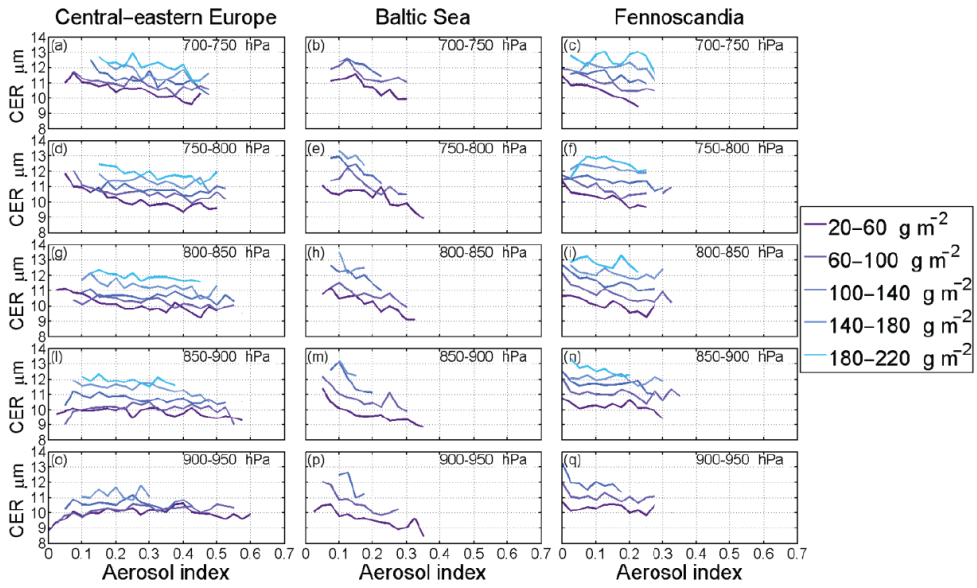

Figure 13: CER as a function of AI, stratified for subranges of CTP and LWP, for the three subregions. These three areas have generally different aerosol conditions:Central-eastern Europe has the highest values of aerosol loading with an overall AI and AOD mean value of 0.29 ± 0.03 (regional mean ± standard deviation), and 0.22 ± 0.02 respectively. The Baltic Sea presents a mean value of 0.20 ± 0.02 and 0.16 ± 0.02 for AI and AOD respectively, and the Fennoscandia the has the lowest values for both AOD (0.14 ± 0.01) and AI (0.16 ± 0.01). The legend on the right of the figure lists the LWP bins.

By using the CDNC as the cloud properties considered in Eq.9, it is possible to isolate the microphysical component of the ACI without the need for constraining the liquid water path. This approach was adopted in **Paper IV** where estimates of ACI on a global scale were computed using CDNC and AI from COSP-MODIS simulated and MODIS retrieval observations. The ACI estimates showed good agreement between the three models and, even more important, with ACI derived from MODIS observations. ACI from the model results is generally positive suggesting that changes in AI are connected with an increase of CDNC regardless of the season. However, negative ACI values were found during the winter months from MODIS observations, possibly caused by limitations intrinsic in the nature of satellite observations.

5. Review of publications and author's contribution

Paper I **Saponaro, G.**, Kolmonen, P., Karhunen, J., Tamminen, J., and de Leeuw, G., A neural network algorithm for cloud fraction estimation using NASA-Aura OMI VIS radiance measurements, *Atmos. Meas. Tech.*, 6, 2301–2309, 2013.

Overview: A study on the applicability of two artificial neural network (ANN) algorithms for estimating cloud fraction. The implemented method revealed being a time effective and automatic approach as oppose to a combination of several tests.

Author's contribution: I implemented the ANN algorithms, collected and processed the MODIS and OMI data for training, testing and validating the ANNs, all of the coding for data processing, and analysed the results. I wrote the text and collated the co-authors comments and revisions.

Paper II Preißler, J., Martucci, G., **Saponaro, G.**, Ovadnevaite, J., Vaishya, A., Kolmonen, P., Cerburis, D., Sogacheva, L., de Leeuw, G. and O'Dowd, C., Six years of surface remote sensing of stratiform warm clouds in marine and continental air over Mace Head, Ireland, *J. Geophys. Res. Atmos.*, 121, 14, 538–14, 557, 2016.

Overview: A long term analysis of cloud properties collected from the CloudNet station located in Mace Head, Ireland. The cloud data was used as input to the SYRSOC algorithm and the derived cloud parameters were compared to satellite observations. Ground-based cloud observations were also studied in function of air masses.

Author's contribution: I contributed to the study by collecting the cloud data from MODIS Collection 6 Level 2 and post-processed it to enable a robust comparison with the ground-based measurements of warm stratiform clouds. I helped in the related data interpretation and wrote the part of text concerning the MODIS observations.

Paper III **Saponaro, G.**, Kolmonen, P., Sogacheva, L., Rodriguez, E., Virtanen, T. and de Leeuw, G., Estimates of the aerosol indirect effect over the Baltic Sea region derived from 12 years of MODIS observations, *Atmos. Chem. Phys.*, 17, 4, 3133–3143, 2017.

Overview: A study on the aerosol indirect effect of aerosols on cloud properties using 12 years of MODIS observations. The study focused on the Baltic Sea region which includes the relatively clean Fennoscandia and the more polluted central-eastern Europe, thus enabling the observation of the effect of different aerosol concentrations on clouds.

Author's contribution: I carried out the design of the study and I chose the methods and metrics. I carried out the data selection, processing and analysis. I wrote the text and collated the co-authors comments and revisions.

Paper IV **Saponaro, G.**, Sporre, M. K., Neubauer, D., Kokkola, H., Kolmonen, P., Sogacheva, L., Arola, A., de Leeuw, G., Karset, I. H. H., Laaksonen, A., Lohmann, U., Evaluation of aerosol and cloud properties in three climate models using MODIS observations and its corresponding COSP simulator, and their application in aerosol-cloud interaction, *Atmos. Chem. Phys. Discussions*

Overview: An evaluation of cloud and aerosol properties simulated by a satellite simulator implemented in three climate models with MODIS observations. The modelling diagnostics and MODIS observations were also used to infer the ACI on a global scale.

Author's contribution: I carried out the design of the study, the analysis of the data and I wrote the text. The modelling data, and the corresponding descriptive sections of the models, were provided by M. Sporre, D. Neubauer and H. Kokkola. I wrote the text and collated the co-authors interpretation of the results, comments and revisions.

6. Conclusions

One main point of this thesis is the use of cloud products from different data sources to evaluate how well they compare, and how they can be used together for climate studies. I mainly focused on liquid warm homogeneous low-level clouds, except in **Paper IV** where ice clouds were also considered.
Paper I and **Paper IV** focused on the evaluation of cloud properties on a global scale. The OMI cloud fraction determined by the two artificial neural networks developed in **Paper I** showed overall good results in comparison to the MODIS cloud fraction, except over bright surfaces (i.e. snow or desert). These areas are usually critical for retrieval algorithms of atmospheric properties as higher surface reflectances can be misinterpreted as aerosol or cloud signals. In an attempt to mitigate this issue, transparent clouds were discarded from the analysis carried in **Paper II** to **Paper IV**.
In **Paper IV** a large difference was found in the two available MODIS cloud fraction products due to the different treatment of partly cloudy pixels which potentially can undermine the robustness of the evaluation of data products if not taken into consideration. The COSP-MODIS satellite simulator used in **Paper IV** avoid the issues related to scale and definition intrinsic in model-model and model-observation comparison and allow a direct evaluation of satellite and COSP diagnostics. However, the simulator diagnostics were not solely used to enable a model-satellite comparison but they were interpreted carefully also to understand the limits and deficiencies between different model set-ups.

The second aim of the thesis was to apply the above mentioned data for assessing the ACI for liquid warm homogeneous clouds on a local scale (**Paper II**), on a regional scale (**Paper III**) and globally (**Paper IV**). The aerosol and cloud observations collected over longer periods of time varying from 6 years in **Paper II** up to 12 years in **Paper III** lead to more statistically and qualitative robust ACI values than the one year data used in **Paper IV**. Implications of ACI were observable by analyzing the spatial distributions, vertical profiles and air masses of the observed atmospheric variables.
The quantification of clouds and of aerosol–cloud interactions remains a challenge. Global climate models are the tool for climate prediction and observations (satellite and surface-based) are used to evaluate the performances of models. On one hand, climate models and satellite are strategic to simulate and observe the relevant atmospheric processes. However, their estimates come with a low confidence because cloud and aerosol properties vary at scales significantly smaller than those resolved both in climate models and observed by satellites. On the other hand, fine scale models and ground-based observation provide high confidence, yet lack the connection with global scale processes.

Future work should aim at coordinating the modelling and observation (satellite and surface-based) communities toward a joint effort to design large-scale activities. Climate models should be improved in their representation of clouds (especially mixed- and ice- clouds) and tested with higher spatial resolution models. The model parametrization capabilities should be tested and evaluated in locations where models indicate sensible mutual interaction between aerosols and clouds, over a range of meteorological and aerosol conditions, and in conjunction with observations.

References

Ackerman, S., Strabala, K., P., M., Frey, R., Moeller, C., and Gumley, L.: Discriminating clear-sky from cloud with MODIS algorithm theoretical basis document (MOD35, in: MODIS Cloud Mask Team, Cooperative Institute for Meteorological Satellite Studies, University of Wisconsin, 2010.

Ackerman, S. A., Strabala, K. I., Menzel, W. P., Frey, R. A., Moeller, C. C., and Gumley, L. E.: Discriminating clear sky from clouds with MODIS, Journal of Geophysical Research: Atmospheres, 103, 32 141–32 157, https://doi.org/10.1029/1998JD200032, URL https://agupubs.onlinelibrary.wiley.com/doi/abs/10.1029/1998JD200032, 1998.

Aebi, C., Gröbner, J., Kämpfer, N., and Vuilleumier, L.: Cloud radiative effect, cloud fraction and cloud type at two stations in Switzerland using hemispherical sky cameras, Atmospheric Measurement Techniques, 10, 4587–4600, https://doi.org/10.5194/amt-10-4587-2017, URL https://www.atmos-meas-tech.net/10/4587/2017/, 2017.

Aitken, J.: XII.—On Dust, Fogs, and Clouds, Transactions of the Royal Society of Edinburgh, 30, 337–368, https://doi.org/10.1017/S0080456800029069, 1881.

Albrecht, B. A.: Aerosols, Cloud Microphysics, and Fractional Cloudiness, Science, 245, 1227–1230, https://doi.org/10.1126/science.245.4923.1227, URL http://science.sciencemag.org/content/245/4923/1227, 1989.

Aleksandrova, M., Gulev, S. K., and Belyaev, K.: Probability Distribution for the Visually Observed Fractional Cloud Cover over the Ocean, Journal of Climate, 31, 3207–3232, https://doi.org/10.1175/JCLI-D-17-0317.1, URL https://doi.org/10.1175/JCLI-D-17-0317.1, 2018.

Andreae, M. O.: Correlation between cloud condensation nuclei concentration and aerosol optical thickness in remote and polluted regions, Atmospheric Chemistry and Physics, 9, 543–556, https://doi.org/10.5194/acp-9-543-2009, URL https://www.atmos-chem-phys.net/9/543/2009/, 2009.

Ban-Weiss, G. A., Jin, L., Bauer, S. E., Bennartz, R., Liu, X., Zhang, K., Ming, Y., Guo, H., and Jiang, J. H.: Evaluating clouds, aerosols, and their interactions in three global climate models using satellite simulators and

observations, Journal of Geophysical Research: Atmospheres, 119, 10,876–10,901, https://doi.org/10.1002/2014JD021722, URL https://agupubs.onlinelibrary.wiley.com/doi/abs/10.1002/2014JD021722, 2014.

Bellouin, N.: AEROSOLS | Climatology of Tropospheric Aerosols, in: Encyclopedia of Atmospheric Sciences (Second Edition), edited by North, G. R., Pyle, J., and Zhang, F., pp. 76 – 85, Academic Press, Oxford, second edition edn., https://doi.org/https://doi.org/10.1016/B978-0-12-382225-3.00054-2, URL http://www.sciencedirect.com/science/article/pii/B9780123822253000542, 2015.

Bellouin, N. and Haywood, J.: AEROSOLS | Climatology of Tropospheric Aerosols, in: Encyclopedia of Atmospheric Sciences (Second Edition), edited by North, G. R., Pyle, J., and Zhang, F., pp. 40 – 47, Academic Press, Oxford, second edition edn., https://doi.org/https://doi.org/10.1016/B978-0-12-382225-3.00051-7, URL http://www.sciencedirect.com/science/article/pii/B9780123822253000517, 2015.

Bellouin, N., Quaas, J., Gryspeerdt, E., Kinne, S., Stier, P., Watson-Parris, D., Boucher, O., Carslaw, K., Christensen, M., Daniau, A.-L., Dufresne, J.-L., Feingold, G., Fiedler, S., Forster, P., Gettelman, A., Haywood, J., Lohmann, U., Malavelle, F., Mauritsen, T., McCoy, D., Myhre, G., Mülmenstädt, J., Neubauer, D., Possner, A., Rugenstein, M., Sato, Y., Schulz, M., Schwartz, S., Sourdeval, O., Storelvmo, T., Toll, V., Winker, D., and Stevens, B.: Bounding global aerosol radiative forcing of climate change, Reviews of Geophysics, https://doi.org/10.1029/2019RG000660, URL https://agupubs.onlinelibrary.wiley.com/doi/abs/10.1029/2019RG000660, 2019.

Bennartz, R.: Global assessment of marine boundary layer cloud droplet number concentration from satellite, Journal of Geophysical Research: Atmospheres, 112, https://doi.org/10.1029/2006JD007547, URL https://agupubs.onlinelibrary.wiley.com/doi/abs/10.1029/2006JD007547, 2007.

Bennartz, R. and Rausch, J.: Global and regional estimates of warm cloud droplet number concentration based on 13 years of AQUA-MODIS observations, Atmospheric Chemistry and Physics, 17, 9815–9836, https://doi.org/10.5194/acp-17-9815-2017, URL https://www.atmos-chem-phys.net/17/9815/2017/, 2017.

Bodas-Salcedo, A., Webb, M. J., Bony, S., Chepfer, H., Dufresne, J.-L., Klein, S. A., Zhang, Y., Marchand, R., Haynes, J. M., Pincus, R., and John,

V. O.: COSP: Satellite simulation software for model assessment, Bulletin of the American Meteorological Society, 92, 1023–1043, https://doi.org/10.1175/2011BAMS2856.1, URL https://doi.org/10.1175/2011BAMS2856.1, 2011.

Bohren, C. F. and Huffman, D. R.: Absorption and Scattering of Light by Small Particles, John Wiley Sons, Ltd, https://doi.org/10.1002/9783527618156.ch1, URL https://onlinelibrary.wiley.com/doi/abs/10.1002/9783527618156.ch1, 2007.

Borg, L. A. and Bennartz, R.: Vertical structure of stratiform marine boundary layer clouds and its impact on cloud albedo, Geophysical Research Letters, 34, https://doi.org/10.1029/2006GL028713, URL https://agupubs.onlinelibrary.wiley.com/doi/abs/10.1029/2006GL028713, 2007.

Boucher, O. and Quaas, J.: Water vapour affects both rain and aerosol optical depth, Nature Geoscience, 6, https://doi.org/10.1038/ngeo1692, URL https://doi.org/10.1038/ngeo1692, 2007.

Boucher, O., Randall, D., Artaxo, P., Bretherton, C., Feingold, G., Forster, P., Kerminen, V.-M., Kondo, Y., Liao, H., Lohmann, U., Rasch, P., Satheesh, S., Sherwood, S., Stevens, B., and Zhang, X.: Clouds and Aerosols, chap. 7, p. 571–658, Cambridge University Press, Cambridge, United Kingdom and New York, NY, USA, https://doi.org/10.1017/CBO9781107415324.016, URL www.climatechange2013.org, 2013.

Brenguier, J.-L., Pawlowska, H., and Schüller, L.: Cloud microphysical and radiative properties for parameterization and satellite monitoring of the indirect effect of aerosol on climate, Journal of Geophysical Research: Atmospheres, 108, https://doi.org/10.1029/2002JD002682, URL https://agupubs.onlinelibrary.wiley.com/doi/abs/10.1029/2002JD002682, 2003.

Chepfer, H., Bony, S., Winker, D., Cesana, G., Dufresne, J. L., Minnis, P., Stubenrauch, C. J., and Zeng, S.: The GCM-Oriented CALIPSO Cloud Product (CALIPSO-GOCCP), Journal of Geophysical Research: Atmospheres, 115, https://doi.org/10.1029/2009JD012251, URL https://agupubs.onlinelibrary.wiley.com/doi/abs/10.1029/2009JD012251, 2010.

Cho, H.-M., Zhang, Z., Meyer, K., Lebsock, M., Platnick, S., Ackerman, A. S., Di Girolamo, L., C.-Labonnote, L., Cornet, C., Riedi, J.,

and Holz, R. E.: Frequency and causes of failed MODIS cloud property retrievals for liquid phase clouds over global oceans, Journal of Geophysical Research: Atmospheres, 120, 4132–4154, https://doi.org/10.1002/2015JD023161, URL https://agupubs.onlinelibrary.wiley.com/doi/abs/10.1002/2015JD023161, 2015.

Christensen, J., Krishna, K. K., Aldrian, E., An, S.-I., Cavalcanti, I., de Castro, M., Dong, W., Goswami, P., Hall, A., Kanyanga, J., Kitoh, A., Kossin, J., Lau, N.-C., Renwick, J., Stephenson, D., Xie, S.-P., and Zhou, T.: Climate Phenomena and their Relevance for Future Regional Climate Change, chap. 14, p. 1217–1308, Cambridge University Press, Cambridge, United Kingdom and New York, NY, USA, https://doi.org/10.1017/CBO9781107415324.028, URL www.climatechange2013.org, 2013.

Collins, M., Knutti, R., Arblaster, J., Dufresne, J.-L., Fichefet, T., Friedlingstein, P., Gao, X., Gutowski, W., Johns, T., Krinner, G., Shongwe, M., Tebaldi, C., Weaver, A., and Wehner, M.: Long-term Climate Change: Projections, Commitments and Irreversibility, book section 12, p. 1029–1136, Cambridge University Press, Cambridge, United Kingdom and New York, NY, USA, https://doi.org/10.1017/CBO9781107415324.024, URL www.climatechange2013.org, 2013.

DeMott, P. J., Rogers, D. C., and Kreidenweis, S. M.: The susceptibility of ice formation in upper tropospheric clouds to insoluble aerosol components, Journal of Geophysical Research: Atmospheres, 102, 19 575–19 584, https://doi.org/10.1029/97JD01138, URL https://agupubs.onlinelibrary.wiley.com/doi/abs/10.1029/97JD01138, 1997.

Dhar, P., Banik, T., De, B. K., Gogoi, M. M., Babu, S. S., and Guha, A.: Study of aerosol types and seasonal sources using wavelength dependent Ångström exponent over North-East India: Ground-based measurement and satellite remote sensing, Advances in Space Research, 62, 1049 – 1064, https://doi.org/https://doi.org/10.1016/j.asr.2018.06.017, URL http://www.sciencedirect.com/science/article/pii/S0273117718304836, 2018.

Draxler, R. R. and Rolph, G. D.: HYSPLIT (HYbrid Single-Particle Lagrangian Integrated Trajectory) Model access via NOAA ARL READYWebsite, URL https://ready.arl.noaa.gov/HYSPLIT.php, 2014.

Eresmaa, R.: Imager-assisted cloud detection for assimilation of Infrared Atmospheric Sounding Interferometer radiances, Quarterly Journal of

the Royal Meteorological Society, 140, 2342–2352, https://doi.org/10.1002/qj.2304, URL https://rmets.onlinelibrary.wiley.com/doi/abs/10.1002/qj.2304, 2014.

Feingold, G., Eberhard, W. L., Veron, D. E., and Previdi, M.: First measurements of the Twomey indirect effect using ground-based remote sensors, Geophysical Research Letters, 30, https://doi.org/10.1029/2002GL016633, URL https://agupubs.onlinelibrary.wiley.com/doi/abs/10.1029/2002GL016633, 2003.

Filonchyk, M., Yan, H. L., Zhang, Z.and Yang, S., Li, W., and Li, Y.: Combined use of satellite and surface observations to study aerosol optical depth in different regions of China, Nature: Scientific Reports, 9, https://doi.org/10.1038/s41598-019-42466-6, URL https://doi.org/10.1038/s41598-019-42466-6, 2019.

Flato, G., Marotzke, J., Abiodun, B., Braconnot, P., Chou, S., Collins, W., Cox, P., Driouech, F., Emori, S., Eyring, V., Forest, C., Gleckler, P., Guilyardi, E., Jakob, C., Kattsov, V., Reason, C., and Rummukainen, M.: Evaluation of Climate Models, book section 9, p. 741–866, Cambridge University Press, Cambridge, United Kingdom and New York, NY, USA, https://doi.org/10.1017/CBO9781107415324.020, URL www.climatechange2013.org, 2013.

Forster, P.and Ramaswamy, V., Artaxo, P., Berntsen, T., Betts, R., Fahey, D., Haywood, J., Lean, J., Lowe, D., Myhre, G., Nganga, J., Prinn, R.and Raga, G., Schulz, M., and Van Dorland, R.: Changes in Atmospheric Constituents and in Radiative Forcing, book section 7, p. 131–217, Cambridge University Press, Cambridge, United Kingdom and New York, NY, USA, 2007.

Go, S., Kim, M., Kim, J., Park, S. S., Jeong, U., and Choi, M.: Detection of Absorbing Aerosol Using Single Near-UV Radiance Measurements from a Cloud and Aerosol Imager, Remote Sensing, 9, https://doi.org/10.3390/rs9040378, URL https://www.mdpi.com/2072-4292/9/4/378, 2017.

Goldblatt, C. and J. Zahnle, K.: Clouds and the Faint Young Sun Paradox, Climate of The Past - CLIM PAST, 6, https://doi.org/10.5194/cp-7-203-2011, 2011.

Grandey, B. S., Stier, P., and Wagner, T. M.: Investigating relationships between aerosol optical depth and cloud fraction using satellite, aerosol reanalysis and general circulation model data, Atmospheric Chemistry and

Physics, 13, 3177–3184, https://doi.org/10.5194/acp-13-3177-2013, URL https://www.atmos-chem-phys.net/13/3177/2013/, 2013.

Grosvenor, D. P. and Wood, R.: The effect of solar zenith angle on MODIS cloud optical and microphysical retrievals within marine liquid water clouds, Atmospheric Chemistry and Physics, 14, 7291–7321, https://doi.org/10.5194/acp-14-7291-2014, URL https://www.atmos-chem-phys.net/14/7291/2014/, 2014.

Grosvenor, D. P., Sourdeval, O., Zuidema, P., Ackerman, A., Alexandrov, M. D., Bennartz, R., Boers, R., Cairns, B., Chiu, J. C., Christensen, M., Deneke, H., Diamond, M., Feingold, G., Fridlind, A., Hünerbein, A., Knist, C., Kollias, P., Marshak, A., McCoy, D., Merk, D., Painemal, D., Rausch, J., Rosenfeld, D., Russchenberg, H., Seifert, P., Sinclair, K., Stier, P., van Diedenhoven, B., Wendisch, M., Werner, F., Wood, R., Zhang, Z., and Quaas, J.: Remote Sensing of Droplet Number Concentration in Warm Clouds: A Review of the Current State of Knowledge and Perspectives, Reviews of Geophysics, 56, 409–453, https://doi.org/10.1029/2017RG000593, URL https://agupubs.onlinelibrary.wiley.com/doi/abs/10.1029/2017RG000593, 2018.

Gryspeerdt, E., Stier, P., and Grandey, B. S.: Cloud fraction mediates the aerosol optical depth-cloud top height relationship, Geophysical Research Letters, 41, 3622–3627, https://doi.org/10.1002/2014GL059524, URL https://agupubs.onlinelibrary.wiley.com/doi/abs/10.1002/2014GL059524, 2014.

Gryspeerdt, E., Quaas, J., and Bellouin, N.: Constraining the aerosol influence on cloud fraction, Journal of Geophysical Research: Atmospheres, 121, 3566–3583, https://doi.org/10.1002/2015JD023744, URL https://agupubs.onlinelibrary.wiley.com/doi/abs/10.1002/2015JD023744, 2016.

Gryspeerdt, E., Quaas, J., Ferrachat, S., Gettelman, A., Ghan, S., Lohmann, U., Morrison, H., Neubauer, D., Partridge, D. G., Stier, P., Takemura, T., Wang, H., Wang, M., and Zhang, K.: Constraining the instantaneous aerosol influence on cloud albedo, Proceedings of the National Academy of Sciences, 114, 4899–4904, https://doi.org/10.1073/pnas.1617765114, URL https://www.pnas.org/content/114/19/4899, 2017.

Hagolle, O., Huc, M., Villa Pascual, D., and G., D.: A multi-temporal method for cloud detection, applied to FORMOSAT-2, VENµS,

LANDSAT and SENTINEL-2 images, Remote Sensing of Environment, 114, 1747 – 1755, https://doi.org/https://doi.org/10.1016/j.rse.2010.03.002, URL http://www.sciencedirect.com/science/article/pii/S0034425710000908, 2010.

Han, Q., Rossow, W. B., Chou, J., and Welch, R. M.: Global Survey of the Relationships of Cloud Albedo and Liquid Water Path with Droplet Size Using ISCCP, Journal of Climate, 11, 1516–1528, https://doi.org/10.1175/1520-0442(1998)011<1516:GSOTRO>2.0.CO;2, URL https://doi.org/10.1175/1520-0442(1998)011<1516:GSOTRO>2.0.CO;2, 1998.

Hang, Y., L'Ecuyer, T. S., Henderson, D. S., Matus, A. V., and Wang, Z.: Reassessing the Effect of Cloud Type on Earth's Energy Balance in the Age of Active Spaceborne Observations. Part II: Atmospheric Heating, Journal of Climate, 32, 6219–6236, https://doi.org/10.1175/JCLI-D-18-0754.1, URL https://doi.org/10.1175/JCLI-D-18-0754.1, 2019.

Hansen, J. E. and Travis, L. D.: Light scattering in planetary atmospheres, Space Science Reviews, 16, 527–610, https://doi.org/10.1007/BF00168069, URL https://doi.org/10.1007/BF00168069, 1974.

Hartmann, D. L.: The Radiative Effect of Clouds on Climate, in: Aerosol-Cloud-Climate Interactions, edited by Hobbs, P., pp. 151–170, Academic Press, 1993.

Heidinger, A. K., Evan, A. T., Foster, M. J., and Walther, A.: A Naive Bayesian Cloud-Detection Scheme Derived from CALIPSO and Applied within PATMOS-x, Journal of Applied Meteorology and Climatology, 51, 1129–1144, https://doi.org/10.1175/JAMC-D-11-02.1, URL https://doi.org/10.1175/JAMC-D-11-02.1, 2012.

Hoesly, R. M., Smith, S. J., Feng, L., Klimont, Z., Janssens-Maenhout, G., Pitkanen, T., Seibert, J. J., Vu, L., Andres, R. J., Bolt, R. M., Bond, T. C., Dawidowski, L., Kholod, N., Kurokawa, J.-I., Li, M., Liu, L., Lu, Z., Moura, M. C. P., O'Rourke, P. R., and Zhang, Q.: Historical (1750–2014) anthropogenic emissions of reactive gases and aerosols from the Community Emissions Data System (CEDS), Geoscientific Model Development, 11, 369–408, https://doi.org/10.5194/gmd-11-369-2018, URL https://www.geosci-model-dev.net/11/369/2018/, 2018.

Huang, S., Xiang, J., Du, H., and Cao, X.: Inverse problems in atmospheric science and their application, Journal of Physics: Conference Series, 12, 45–

57, https://doi.org/10.1088/1742-6596/12/1/005, URL https://doi.org/10.1088/2F1742-6596/2F12/2F1/2F005, 2005.

Hubanks, P., Platnick, S., and King, M. Ridgway, B.: MODIS ATBD for Level-3 Global Gridded Atmosphere Products (Collection 006, v4.3), 2018.

Hulley, G. C. and Hook, S. J.: A new methodology for cloud detection and classification with ASTER data, Geophysical Research Letters, 35, https://doi.org/10.1029/2008GL034644, URL https://agupubs.onlinelibrary.wiley.com/doi/abs/10.1029/2008GL034644, 2008.

Jia, H., Ma, X., Quaas, J., Yin, Y., and Qiu, T.: Is positive correlation between cloud droplet effective radius and aerosol optical depth over land due to retrieval artifacts or real physical processes?, Atmospheric Chemistry and Physics, 19, 8879–8896, https://doi.org/10.5194/acp-19-8879-2019, URL https://www.atmos-chem-phys.net/19/8879/2019/, 2019.

Kalberer, M.: AEROSOLS | Aerosol Physics and Chemistry, in: Encyclopedia of Atmospheric Sciences (Second Edition), edited by North, G. R., Pyle, J., and Zhang, F., pp. 23 – 31, Academic Press, Oxford, second edition edn., https://doi.org/https://doi.org/10.1016/B978-0-12-382225-3.00049-9, URL http://www.sciencedirect.com/science/article/pii/B9780123822253000499, 2015.

Kaufman, Y. J. and Koren, I.: Smoke and Pollution Aerosol Effect on Cloud Cover, Science, 313, 655–658, https://doi.org/10.1126/science.1126232, URL http://science.sciencemag.org/content/313/5787/655, 2006.

Kay, J. E., Hillman, B. R., Klein, S. A., Zhang, Y., Medeiros, B., Pincus, R., Gettelman, A., Eaton, B., Boyle, J., Marchand, R., and Ackerman, T. P.: Exposing Global Cloud Biases in the Community Atmosphere Model (CAM) Using Satellite Observations and Their Corresponding Instrument Simulators, Journal of Climate, 25, 5190–5207, https://doi.org/10.1175/JCLI-D-11-00469.1, URL https://doi.org/10.1175/JCLI-D-11-00469.1, 2012.

Kazil, J., Stier, P., Zhang, K., Quaas, J., Kinne, S., O'Donnell, D., Rast, S., Esch, M., Ferrachat, S., Lohmann, U., and Feichter, J.: Aerosol nucleation and its role for clouds and Earth's radiative forcing in the aerosol-climate model ECHAM5-HAM, Atmospheric Chemistry and Physics, 10, 10 733–10 752, https://doi.org/10.5194/acp-10-10733-2010, URL https://www.atmos-chem-phys.net/10/10733/2010/, 2010.

King, M. D., Tsay, S. C., Platnick, S. E., Wang, M., and Liou, K. N.: Cloud retrieval algorithm for MODIS: Optical thickness, effective particle radius, and thermodynamic phase. MODIS Algorithm Theoretical Basis Document, 1997.

Kirtman, B., Power, S., Adedoyin, J., Boer, G., Bojariu, R., Camilloni, I., Doblas-Reyes, F., Fiore, A., Kimoto, M., Meehl, G., Prather, M., Sarr, A., Schär, C., Sutton, R., van Oldenborgh, G., Vecchi, G., and Wang, H.: Near-term Climate Change: Projections and Predictability, book section 11, p. 953–1028, Cambridge University Press, Cambridge, United Kingdom and New York, NY, USA, https://doi.org/10.1017/CBO9781107415324.023, URL www.climatechange2013.org, 2013.

Koffi, B., Schulz, M., Bréon, F.-M., Dentener, F., Steensen, B. M., Griesfeller, J., Winker, D., Balkanski, Y., Bauer, S. E., Bellouin, N., Berntsen, T., Bian, H., Chin, M., Diehl, T., Easter, R., Ghan, S., Hauglustaine, D. A., Iversen, T., Kirkevåg, A., Liu, X., Lohmann, U., Myhre, G., Rasch, P., Seland, ., Skeie, R. B., Steenrod, S. D., Stier, P., Tackett, J., Takemura, T., Tsigaridis, K., Vuolo, M. R., Yoon, J., and Zhang, K.: Evaluation of the aerosol vertical distribution in global aerosol models through comparison against CALIOP measurements: AeroCom phase II results, Journal of Geophysical Research: Atmospheres, 121, 7254–7283, https://doi.org/10.1002/2015JD024639, URL https://agupubs.onlinelibrary.wiley.com/doi/abs/10.1002/2015JD024639, 2016.

Koren, I., Altaratz, O., , Remer, L. A., Feingold, G., Martins, J. V., and Heiblum, R. H.: How small is a small cloud?, Atmospheric Chemistry and Physics, 8, 3855–3864, https://doi.org/10.5194/acp-8-3855-2008, URL https://www.atmos-chem-phys.net/8/3855/2008/, 2008.

Koren, I., Oreopoulos, L., Feingold, G., Remer, L. A., and Altaratz, O.: Aerosol-induced intensification of rain from the tropics to the mid-latitudes, Nature Geoscience, 4, https://doi.org/10.1038/ngeo1364, URL https://doi.org/10.1038/ngeo1364, 2012.

Kristiansen, N. I., Stohl, A., and Wotawa, G.: Atmospheric removal times of the aerosol-bound radionuclides ^{137}Cs and ^{131}I measured after the Fukushima Dai-ichi nuclear accident ndash; a constraint for air quality and climate models, Atmospheric Chemistry and Physics, 12, 10 759–10 769, https://doi.org/10.5194/acp-12-10759-2012, URL https://www.atmos-chem-phys.net/12/10759/2012/, 2012.

Kulmala, M., Korhonen, P., Vesala, T., Hansson, H.-C., Noone, K., and Svenningsson, B.: The effect of hygroscopicity on cloud droplet formation, Tellus B: Chemical and Physical Meteorology, 48, 347–360, https://doi.org/10.3402/tellusb.v48i3.15903, URL https://doi.org/10.3402/tellusb.v48i3.15903, 1996.

Kulmala, M., , Petäjä, T., nieminen, T., Sipilä, M., Manninen, H. E., Lehtipalo, K., Dal Maso, M., Aalto, P. P., Junninen, H., Paasonen, P., Riipinen, I., Lehtinen, K. E. J., Laaksonen, A., and Kerminen, V.-M.: Measurement of the nucleation of atmospheric aerosol particles, Nature Protocols, 7, https://doi.org/10.1038/nprot.2012.091, URL https://doi.org/10.1038/nprot.2012.091, 2012.

Kulmala, M., Kontkanen, J., Junninen, H., Lehtipalo, K., Manninen, H. E., Nieminen, T., Petäjä, T., Sipilä, M., Schobesberger, S., Rantala, P., Franchin, A., Jokinen, T., Järvinen, E., Äijälä, M., Kangasluoma, J., Hakala, J., Aalto, P. P., Paasonen, P., Mikkilä, J., Vanhanen, J., Aalto, J., Hakola, H., Makkonen, U., Ruuskanen, T., Mauldin, R. L., Duplissy, J., Vehkamäki, H., Bäck, J., Kortelainen, A., Riipinen, I., Kurtén, T., Johnston, M. V., Smith, J. N., Ehn, M., Mentel, T. F., Lehtinen, K. E. J., Laaksonen, A., Kerminen, V.-M., and Worsnop, D. R.: Direct Observations of Atmospheric Aerosol Nucleation, Science, 339, 943–946, https://doi.org/10.1126/science.1227385, URL https://science.sciencemag.org/content/339/6122/943, 2013.

Köhler, H.: The nucleus in and the growth of hygroscopic droplets, Trans. Faraday Soc., 32, 1152–1161, https://doi.org/10.1039/TF9363201152, URL http://dx.doi.org/10.1039/TF9363201152, 1936.

Lack, D. A. and Langridge, J. M.: On the attribution of black and brown carbon light absorption using the Ångström exponent, Atmospheric Chemistry and Physics, 13, 10 535–10 543, https://doi.org/10.5194/acp-13-10535-2013, URL https://www.atmos-chem-phys.net/13/10535/2013/, 2013.

Lamb, D. and Verlinde, J.: Physics and chemistry of clouds, Cambridge University Press, United Kingdom, https://doi.org/10.1017/CBO9780511976377, 2011.

Lee, S. S.: Effect of Aerosol on Circulations and Precipitation in Deep Convective Clouds, Journal of the Atmospheric Sciences, 69, 1957–1974, https://doi.org/10.1175/JAS-D-11-0111.1, URL https://doi.org/10.1175/JAS-D-11-0111.1, 2012.

Levelt, P. F., van den Oord, G. H. J., Dobber, M. R., Malkki, A., Visser, H., de Vries, J., Stammes, P., Lundell, J. O. V., and Saari, H.: The ozone monitoring instrument, IEEE Transactions on Geoscience and Remote Sensing, 44, 1093–1101, https://doi.org/10.1109/TGRS.2006.872333, 2006.

Levy, R., Hsu, C., Sayer, A., Mattoo, S., and Lee, J.: The Collection 6 MODIS aerosol products over land and ocean, https://doi.org/[doi:10.5067/MODIS/MOD04_L2.006;doi:10.5067/MODIS/MYD04_L2.006], 2015.

Levy, R. C., Mattoo, S., Munchak, L. A., Remer, L. A., Sayer, A. M., Patadia, F., and Hsu, N. C.: The Collection 6 MODIS aerosol products over land and ocean, Atmospheric Measurement Techniques, 6, 2989–3034, https://doi.org/10.5194/amt-6-2989-2013, URL https://www.atmos-meas-tech.net/6/2989/2013/, 2013.

Liu, J. and Li, Z.: Significant Underestimation in the Optically Based Estimation of the Aerosol First Indirect Effect Induced by the Aerosol Swelling Effect, Geophysical Research Letters, 45, 5690–5699, https://doi.org/10.1029/2018GL077679, URL https://agupubs.onlinelibrary.wiley.com/doi/abs/10.1029/2018GL077679, 2018.

Lohmann, U.: Aerosol Effects on Clouds and Climate, Space Science Reviews, 125, 129–137, https://doi.org/10.1007/s11214-006-9051-8, URL https://doi.org/10.1007/s11214-006-9051-8, 2006.

Lohmann, U. and Neubauer, D.: The importance of mixed-phase and ice clouds for climate sensitivity in the global aerosol–climate model ECHAM6-HAM2, Atmospheric Chemistry and Physics, 18, 8807–8828, https://doi.org/10.5194/acp-18-8807-2018, URL https://www.atmos-chem-phys.net/18/8807/2018/, 2018.

Lohmann, U., Lüönd, F., and Mahrt, F.: An Introduction to Clouds: From the Microscale to Climate, Cambridge University Press, https://doi.org/10.1017/CBO9781139087513, 2016.

L'Ecuyer, T. S., Hang, Y., Matus, A. V., and Wang, Z.: Reassessing the Effect of Cloud Type on Earth's Energy Balance in the Age of Active Spaceborne Observations. Part I: Top of Atmosphere and Surface, Journal of Climate, 32, 6197–6217, https://doi.org/10.1175/JCLI-D-18-0753.1, URL https://doi.org/10.1175/JCLI-D-18-0753.1, 2019.

Ma, X., Jia, H., Yu, F., and Quaas, J.: Opposite Aerosol Index-Cloud Droplet Effective Radius Correlations Over Major Industrial Regions and Their Adjacent Oceans, Geophysical Research Letters, 45, 5771–5778, https://doi.org/10.1029/2018GL077562, URL https://agupubs.onlinelibrary.wiley.com/doi/abs/10.1029/2018GL077562, 2018.

Mace, G. G., Zhang, Q., Vaughan, M., Marchand, R., Stephens, G., Trepte, C., and Winker, D.: A description of hydrometeor layer occurrence statistics derived from the first year of merged Cloudsat and CALIPSO data, Journal of Geophysical Research: Atmospheres, 114, https://doi.org/10.1029/2007JD009755, URL https://agupubs.onlinelibrary.wiley.com/doi/abs/10.1029/2007JD009755, 2009.

Marchand, R.: ARM and Satellite Cloud Validation, Meteorological Monographs, 57, 30.1–30.11, https://doi.org/10.1175/AMSMONOGRAPHS-D-15-0038.1, URL https://doi.org/10.1175/AMSMONOGRAPHS-D-15-0038.1, 2016.

Martucci, G. and O'Dowd, C. D.: Ground-based retrieval of continental and marine warm cloud microphysics, Atmospheric Measurement Techniques, 4, 2749–2765, https://doi.org/10.5194/amt-4-2749-2011, URL https://www.atmos-meas-tech.net/4/2749/2011/, 2011.

Mie, G.: Beiträge zur Optik trüber Medien, speziell kolloidaler Metallösungen, Annalen der Physik, 330, 377–445, https://doi.org/10.1002/andp.19083300302, URL https://onlinelibrary.wiley.com/doi/abs/10.1002/andp.19083300302, 1908.

Mochida, M., Nishita-Hara, C., Furutani, H., Miyazaki, Y., Jung, J., Kawamura, K., and Uematsu, M.: Hygroscopicity and cloud condensation nucleus activity of marine aerosol particles over the western North Pacific, Journal of Geophysical Research: Atmospheres, 116, https://doi.org/10.1029/2010JD014759, URL https://agupubs.onlinelibrary.wiley.com/doi/abs/10.1029/2010JD014759, 2011.

Moosmüller, H., Chakrabarty, R., and Arnott, W.: Aerosol light absorption and its measurement: A review, Journal of Quantitative Spectroscopy and Radiative Transfer, 110, 844 – 878, https://doi.org/https://doi.org/10.1016/j.jqsrt.2009.02.035, URL http://www.sciencedirect.com/science/article/pii/S0022407309000879, 2009.

Myhre, G., Stordal, F., Johnsrud, M., Kaufman, Y. J., Rosenfeld, D., Storelvmo, T., Kristjansson, J. E., Berntsen, T. K., Myhre, A., and Isaksen, I. S. A.: Aerosol-cloud interaction inferred from MODIS satellite data and global aerosol models, Atmospheric Chemistry and Physics, 7, 3081–3101, https://doi.org/10.5194/acp-7-3081-2007, URL https://www.atmos-chem-phys.net/7/3081/2007/, 2007.

Neubauer, D., Christensen, M. W., Poulsen, C. A., and Lohmann, U.: Unveiling aerosol–cloud interactions – Part 2: Minimising the effects of aerosol swelling and wet scavenging in ECHAM6-HAM2 for comparison to satellite data, Atmospheric Chemistry and Physics, 17, 13 165–13 185, https://doi.org/10.5194/acp-17-13165-2017, URL https://www.atmos-chem-phys.net/17/13165/2017/, 2017.

Neubauer, D., Ferrachat, S., Siegenthaler-Le Drian, C., Stier, P., Partridge, D. G., Tegen, I., Bey, I., Stanelle, T., Kokkola, H., and Lohmann, U.: The global aerosol-climate model ECHAM6.3-HAM2.3 â€“ Part 2: Cloud evaluation, aerosol radiative forcing and climate sensitivity, Geoscientific Model Development Discussions, 2019, 1–52, https://doi.org/10.5194/gmd-2018-307, URL https://www.geosci-model-dev-discuss.net/gmd-2018-307/, 2019.

Nilo, S. T., Romano, F., Cermak, J., Cimini, D., Ricciardelli, E., Cersosimo, A., Di Paola, F., Gallucci, D., Gentile, S., Geraldi, E., Larosa, S., Ripepi, E., and Viggiano, M.: Fog Detection Based on Meteosat Second Generation-Spinning Enhanced Visible and InfraRed Imager High Resolution Visible Channel, Remote Sensing, 10, https://doi.org/10.3390/rs10040541, URL https://www.mdpi.com/2072-4292/10/4/541, 2018.

Ovadnevaite, J., Ceburnis, D., Leinert, S., Dall'Osto, M., Canagaratna, M., O'Doherty, S., Berresheim, H., and O'Dowd, C.: Submicron NE Atlantic marine aerosol chemical composition and abundance: Seasonal trends and air mass categorization, Journal of Geophysical Research: Atmospheres, 119, 11,850–11,863, https://doi.org/10.1002/2013JD021330, URL https://agupubs.onlinelibrary.wiley.com/doi/abs/10.1002/2013JD021330, 2014.

Painemal, D.: Global Estimates of Changes in Shortwave Low-Cloud Albedo and Fluxes Due to Variations in Cloud Droplet Number Concentration Derived From CERES-MODIS Satellite Sensors, Geophysical Research Letters, 45, 9288–9296, https://doi.org/10.1029/

2018GL078880, URL https://agupubs.onlinelibrary.wiley.com/doi/abs/10.1029/2018GL078880, 2018.

Parmes, E., Rauste, Y., Molinier, M., Andersson, K., and Seitsonen, L.: Automatic Cloud and Shadow Detection in Optical Satellite Imagery Without Using Thermal Bands—Application to Suomi NPP VIIRS Images over Fennoscandia, Remote Sensing, 9, https://doi.org/10.3390/rs9080806, URL https://www.mdpi.com/2072-4292/9/8/806, 2017.

Platnick, S., King, M. D., Meyer, K. G.and Wind, G. A. N., Marchant, B., Arnold, G. T., Zhang, Z. B., Hubanks, P. A., Ridgway, B., and Riedi, J.: MODIS Cloud Optical Properties: User Guide for the Collection 6 Level-2 MOD06/MYD06 Product and Associated Level-3 Datasets, Version 1.0, October 2015, URL availableat:http://modis-atmos.gsfc.nasa.gov/_docs/C6MOD06OPUserGuide.pdf(lastaccess:16August2017), 2015.

Platnick, S., Meyer, K. G.and King, M. D., Wind, G., Amarasinghe, N., Marchant, B., Arnold, G. T., Zhang, Z., Hubanks, P. A., Holz, R. E., Yang, P., Ridgway, W. L., and Riedi, J.: The MODIS Cloud Optical and Microphysical Products: Collection 6 Updates and Examples From Terra and Aqua, IEEE Transactions on Geoscience and Remote Sensing, 55, 502–525, https://doi.org/10.1109/TGRS.2016.2610522, 2017.

Platnick, S., Meyer, K. G., King, M. D., Wind, G., Amarasinghe, N., Marchant, B., Arnold, G. T. Zhang, Z. H. P. A., Ridgway, B., and J., R.: MODIS Cloud optical properties: User guide for the Collection 6/6.1 level-2 MOD06/MYD06 product and associated level-3 data sets. Version1.1, Tech. rep., 2018.

Qiu, Y., Zhao, C., Guo, J., and Li, J.: 8-Year ground-based observational analysis about the seasonal variation of the aerosol-cloud droplet effective radius relationship at SGP site, Atmospheric Environment, 164, 139 – 146, https://doi.org/https://doi.org/10.1016/j.atmosenv.2017.06.002, URL http://www.sciencedirect.com/science/article/pii/S1352231017303746, 2017.

Quaas, J., Boucher, O., and Lohmann, U.: Constraining the total aerosol indirect effect in the LMDZ and ECHAM4 GCMs using MODIS satellite data, Atmospheric Chemistry and Physics, 6, 947–955, https://doi.org/10.5194/acp-6-947-2006, URL https://www.atmos-chem-phys.net/6/947/2006/, 2006.

Quaas, J., Stevens, B., Stier, P., and Lohmann, U.: Interpreting the cloud cover - aerosol optical depth relationship found in satellite data using a general circulation model, Atmospheric Chemistry and Physics, 10, 6129–6135, https://doi.org/10.5194/acp-10-6129-2010, URL https://www.atmos-chem-phys.net/10/6129/2010/, 2010.

Rausch, J., Heidinger, A., and Bennartz, R.: Regional assessment of microphysical properties of marine boundary layer cloud using the PATMOS-x dataset, Journal of Geophysical Research: Atmospheres, 115, https://doi.org/10.1029/2010JD014468, URL https://agupubs.onlinelibrary.wiley.com/doi/abs/10.1029/2010JD014468, 2010.

Reutter, P., Su, H., Trentmann, J., Simmel, M., Rose, D., Gunthe, S. S., Wernli, H., Andreae, M. O., and Pöschl, U.: Aerosol- and updraft-limited regimes of cloud droplet formation: influence of particle number, size and hygroscopicity on the activation of cloud condensation nuclei (CCN), Atmospheric Chemistry and Physics, 9, 7067–7080, https://doi.org/10.5194/acp-9-7067-2009, URL https://www.atmos-chem-phys.net/9/7067/2009/, 2009.

Rosenfeld, D.: Aerosol-Cloud Interactions Control of Earth Radiation and Latent Heat Release Budgets, Space Science Reviews, 125, 149–157, https://doi.org/10.1007/s11214-006-9053-6, URL https://doi.org/10.1007/s11214-006-9053-6, 2006.

Rosenfeld, D. and Givati, A.: Evidence of Orographic Precipitation Suppression by Air Pollution–Induced Aerosols in the Western United States, Journal of Applied Meteorology and Climatology, 45, 893–911, https://doi.org/10.1175/JAM2380.1, URL https://doi.org/10.1175/JAM2380.1, 2006.

Rossow, W. B. and Garder, L. C.: Cloud Detection Using Satellite Measurements of Infrared and Visible Radiances for ISCCP, Journal of Climate, 6, 2341–2369, https://doi.org/10.1175/1520-0442(1993)006<2341:CDUSMO>2.0.CO;2, URL https://doi.org/10.1175/1520-0442(1993)006<2341:CDUSMO>2.0.CO;2, 1993.

Seinfeld, J. H. and Pandis, S. N.: Atmospheric Chemistry and Physics: From Air Pollution to Climate Change, John Wiley Sons, Inc., 2 edn., 2006.

Seinfeld, J. H., Bretherton, C., Carslaw, K. S., Coe, H., DeMott, P. J., Dunlea, E. J., Feingold, G., Ghan, S., Guenther, A. B., Kahn, R., Kraucunas, I., Kreidenweis, S. M., Molina, M. J., Nenes, A., Penner, J. E.,

Prather, K. A., Ramanathan, V., Ramaswamy, V., Rasch, P. J., Ravishankara, A. R., Rosenfeld, D., Stephens, G., and Wood, R.: Improving our fundamental understanding of the role of aerosol-cloud interactions in the climate system, Proceedings of the National Academy of Sciences, 113, 5781–5790, https://doi.org/10.1073/pnas.1514043113, URL https://www.pnas.org/content/113/21/5781, 2016.

Shin, S.-K., Tesche, M., Müller, D., and Noh, Y.: Technical note: Absorption aerosol optical depth components from AERONET observations of mixed dust plumes, Atmospheric Measurement Techniques, 12, 607–618, https://doi.org/10.5194/amt-12-607-2019, URL https://www.atmos-meas-tech.net/12/607/2019/, 2019.

Stephens, G. L.: Cloud Feedbacks in the Climate System: A Critical Review, Journal of Climate, 18, 237–273, https://doi.org/10.1175/JCLI-3243.1, URL https://doi.org/10.1175/JCLI-3243.1, 2005.

Stier, P.: Limitations of passive remote sensing to constrain global cloud condensation nuclei, Atmospheric Chemistry and Physics, 16, 6595–6607, https://doi.org/10.5194/acp-16-6595-2016, URL https://www.atmos-chem-phys.net/16/6595/2016/, 2016.

Stjern, C. W., Samset, B. H., Myhre, G., Forster, P. M., Hodnebrog, ., Andrews, T., Boucher, O., Faluvegi, G., Iversen, T., Kasoar, M., Kharin, V., Kirkevåg, A., Lamarque, J.-F., Olivié, D., Richardson, T., Shawki, D., Shindell, D., Smith, C. J., Takemura, T., and Voulgarakis, A.: Rapid Adjustments Cause Weak Surface Temperature Response to Increased Black Carbon Concentrations, Journal of Geophysical Research: Atmospheres, 122, 11,462–11,481, https://doi.org/10.1002/2017JD027326, URL https://agupubs.onlinelibrary.wiley.com/doi/abs/10.1002/2017JD027326, 2017.

Sun, L., Mi, X., Wei, J., Wang, J., Tian, X., Yu, H., and Gan, P.: A cloud detection algorithm-generating method for remote sensing data at visible to short-wave infrared wavelengths, ISPRS Journal of Photogrammetry and Remote Sensing, 124, 70 – 88, https://doi.org/https://doi.org/10.1016/j.isprsjprs.2016.12.005, URL http://www.sciencedirect.com/science/article/pii/S0924271616306189, 2017.

Sun, Q., Miao, C., Duan, Q., Ashouri, H., Sorooshian, S., and Hsu, K.-L.: A Review of Global Precipitation Data Sets: Data Sources, Estimation, and Intercomparisons, Reviews of Geophysics, 56, 79–107, https://doi.org/10.

1002/2017RG000574, URL https://agupubs.onlinelibrary.wiley.com/doi/abs/10.1002/2017RG000574, 2018.

Tegen, I. and Schepanski, K.: Climate Feedback on Aerosol Emission and Atmospheric Concentrations, Current Climate Change Reports, 4, 1–1, https://doi.org/10.1007/s40641-018-0086-1, URL https://doi.org/10.1007/s40641-018-0086-1, 2018.

Tian, P., Cao, X., Zhang, L., Sun, N., Sun, L., Logan, T., Shi, J., Wang, Y., Ji, Y., Lin, Y., Huang, Z., Zhou, T., Shi, Y., and Zhang, R.: Aerosol vertical distribution and optical properties over China from long-term satellite and ground-based remote sensing, Atmospheric Chemistry and Physics, 17, 2509–2523, https://doi.org/10.5194/acp-17-2509-2017, URL https://www.atmos-chem-phys.net/17/2509/2017/, 2017.

Twomey, S.: The Influence of Pollution on the Shortwave Albedo of Clouds, Journal of the Atmospheric Sciences, 34, 1149–1152, https://doi.org/10.1175/1520-0469(1977)034<1149:TIOPOT>2.0.CO;2, URL https://doi.org/10.1175/1520-0469(1977)034<1149:TIOPOT>2.0.CO;2, 1977.

Väisänen, O., Ruuskanen, A., Ylisirniö, A., Miettinen, P., Portin, H., Hao, L., Leskinen, A., Komppula, M., Romakkaniemi, S., Lehtinen, K. E. J., and Virtanen, A.: In-cloud measurements highlight the role of aerosol hygroscopicity in cloud droplet formation, Atmospheric Chemistry and Physics, 16, 10 385–10 398, https://doi.org/10.5194/acp-16-10385-2016, URL https://www.atmos-chem-phys.net/16/10385/2016/, 2016.

Virtanen, T. H., Kolmonen, P., Sogacheva, L., Rodríguez, E., Saponaro, G., and de Leeuw, G.: Collocation mismatch uncertainties in satellite aerosol retrieval validation, Atmospheric Measurement Techniques, 11, 925–938, https://doi.org/10.5194/amt-11-925-2018, URL https://www.atmos-meas-tech.net/11/925/2018/, 2018.

Wallace, J. M. and Hobbs, P.: Atmospheric Science: An Introductory Survey, U.K. Elsevier Inc, 3 edn., 2006.

Webb, M. J., Andrews, T., Bodas-Salcedo, A., Bony, S., Bretherton, C. S., Chadwick, R., Chepfer, H., Douville, H., Good, P., Kay, J. E., Klein, S. A., Marchand, R., Medeiros, B., Siebesma, A. P., Skinner, C. B., Stevens, B., Tselioudis, G., Tsushima, Y., and Watanabe, M.: The Cloud Feedback Model Intercomparison Project (CFMIP) contribution to CMIP6, Geoscientific Model Development, 10, 359–384, https://doi.org/10.

5194/gmd-10-359-2017, URL https://www.geosci-model-dev.net/10/359/2017/, 2017.

Werner, F., Ditas, F., Siebert, H., Simmel, M., Wehner, B., Pilewskie, P., Schmeissner, T., Shaw, R. A., Hartmann, S., Wex, H., Roberts, G. C., and Wendisch, M.: Twomey effect observed from collocated microphysical and remote sensing measurements over shallow cumulus, Journal of Geophysical Research: Atmospheres, 119, 1534–1545, https://doi.org/10.1002/2013JD020131, URL https://agupubs.onlinelibrary.wiley.com/doi/abs/10.1002/2013JD020131, 2014.

Yan, H., Chen, L., Tao, J., Su, L., Huang, J., Han, D., and Yu, C.: Corrections for OMI SO_2 BRD retrievals influenced by row anomalies, Atmospheric Measurement Techniques, 5, 2635–2646, https://doi.org/10.5194/amt-5-2635-2012, URL https://www.atmos-meas-tech.net/5/2635/2012/, 2012.

Yan, Y., Liu, Y., and Lu, J.: Cloud vertical structure, precipitation, and cloud radiative effects over Tibetan Plateau and its neighboring regions, Journal of Geophysical Research: Atmospheres, 121, 5864–5877, https://doi.org/10.1002/2015JD024591, URL https://agupubs.onlinelibrary.wiley.com/doi/abs/10.1002/2015JD024591, 2016.

Yang, W., Marshak, A., Várnai, T., and Wood, R.: CALIPSO observations of near-cloud aerosol properties as a function of cloud fraction, Geophysical Research Letters, 41, 9150–9157, https://doi.org/10.1002/2014GL061896, 2014.

Zhang, Z., Ackerman, A. S., Feingold, G., Platnick, S., Pincus, R., and Xue, H.: Effects of cloud horizontal inhomogeneity and drizzle on remote sensing of cloud droplet effective radius: Case studies based on large-eddy simulations, Journal of Geophysical Research: Atmospheres, 117, n/a–n/a, https://doi.org/10.1029/2012JD017655, URL http://dx.doi.org/10.1029/2012JD017655, d19208, 2012.

Zhou, X., Ackerman, A. S., Fridlind, A. M., Wood, R., and Kollias, P.: Impacts of solar-absorbing aerosol layers on the transition of stratocumulus to trade cumulus clouds, Atmospheric Chemistry and Physics, 17, 12 725–12 742, https://doi.org/10.5194/acp-17-12725-2017, URL https://www.atmos-chem-phys.net/17/12725/2017/, 2017.

Zhu, L., Suomalainen, J., Liu, J., Hyyppä, J., Kaartinen, H., and Haggren, H.: A Review: Remote Sensing Sensors, in: Multi-purposeful Application of

Geospatial Data, edited by Rustamov, R. B., Hasanova, S., and Zeynalova, M. H., chap. 2, IntechOpen, Rijeka, https://doi.org/10.5772/intechopen.71049, URL https://doi.org/10.5772/intechopen.71049, 2018.

Zhu, Y., Rosenfeld, D., Yu, X., and Li, Z.: Separating aerosol microphysical effects and satellite measurement artifacts of the relationships between warm rain onset height and aerosol optical depth, Journal of Geophysical Research: Atmospheres, 120, 7726–7736, https://doi.org/10.1002/2015JD023547, URL https://agupubs.onlinelibrary.wiley.com/doi/abs/10.1002/2015JD023547, 2015.

Zhu, Z. and Woodcock, C. E.: Automated cloud, cloud shadow, and snow detection in multitemporal Landsat data: An algorithm designed specifically for monitoring land cover change, Remote Sensing of Environment, 152, 217 – 234, https://doi.org/https://doi.org/10.1016/j.rse.2014.06.012, URL http://www.sciencedirect.com/science/article/pii/S0034425714002259, 2014.

Zotter, P., Herich, H., Gysel, M., El-Haddad, I., Zhang, Y., Močnik, G., Hüglin, C., Baltensperger, U., Szidat, S., and Prévôt, A. S. H.: Evaluation of the absorption Ångström exponents for traffic and wood burning in the Aethalometer-based source apportionment using radiocarbon measurements of ambient aerosol, Atmospheric Chemistry and Physics, 17, 4229–4249, https://doi.org/10.5194/acp-17-4229-2017, URL https://www.atmos-chem-phys.net/17/4229/2017/, 2017.

Ångström, A.: On the Atmospheric Transmission of Sun Radiation and on Dust in the Air, Geografiska Annaler, 11, 156–166, https://doi.org/10.1080/20014422.1929.11880498, URL https://doi.org/10.1080/20014422.1929.11880498, 1929.